Final Report

Estimating Traffic Stream Density Using Connected Vehicle Data

Mohammad A. Aljamal, Ph.D.
Virginia Tech Transportation Institute
3500 Transportation Research Plaza
Blacksburg, VA 24061
m7md92@vt.edu

Hossam M. Abdelghaffar, Ph.D.
Virginia Tech Transportation Institute
3500 Transportation Research Plaza
Blacksburg, VA 24061
hossamvt@vt.edu

Hesham A. Rakha, Ph.D., P.Eng.
Charles E. Via, Jr. Department of Civil and Environmental Engineering
Virginia Polytechnic Institute and State University
3500 Transportation Research Plaza
Blacksburg, VA 24061
Phone: (540) 231-1505
Fax: (540) 231-1555

hrakha@vt.edu

Date
April 2021

Prepared for the Urban Mobility & Equity Center, Morgan State University, CBEIS 327, 1700 E. Coldspring Lane, Baltimore, MD 21251

ACKNOWLEDGMENT

This research was funded by the Urban Mobility & Equity Center at Morgan State University and the University Transportation Center(s) Program of the U.S. Department of Transportation.

Disclaimer

The contents of this report reflect the views of the authors, who are responsible for the facts and the accuracy of the information presented herein. This document is disseminated under the sponsorship of the U.S. Department of Transportation's University Transportation Centers Program, in the interest of information exchange. The U.S. Government assumes no liability for the contents or use thereof.

1. Report No. UMEC-030	**2. Government Accession No.**	**3. Recipient's Catalog No.**
4. Title and Subtitle Estimating Traffic Stream Density Using Connected Vehicle Data		**5. Report Date** April 2021
		6. Performing Organization Code
7. Author(s) Mohammad A. Aljamal (ORCID # 0000-0003-4251-1899) Hossam M. Abdelghaffar (ORCID # 0000-0003-4396-5913) Hesham A. Rakha (ORCID # 0000-0002-5845-2929)		**8. Performing Organization Report No.**
9. Performing Organization Name and Address Virginia Tech Transportation Institute 3500 Transportation Research Road Blacksburg, VA 24061		**10. Work Unit No.**
		11. Contract or Grant No. 69A43551747123
12. Sponsoring Agency Name and Address US Department of Transportation Office of the Secretary-Research UTC Program, RDT-30 1200 New Jersey Ave., SE Washington, DC 20590		**13. Type of Report and Period Covered** Final May 2020 - April 2021
		14. Sponsoring Agency Code

15. Supplementary Notes

16. Abstract

The macroscopic traffic stream density is crucial in advanced traffic management systems. However, measuring the traffic density in the field is difficult since it is categorized as a spatial measurement. In this report, several estimation approaches are developed to estimate the traffic stream density on signalized links using connected vehicle (CV) data. First, the report introduces a novel variable estimation interval that allows for higher estimation precision, as the updating time interval always contains a fixed number of CVs. After that, the report develops a linear Kalman filter (KF), a linear adaptive KF (AKF), and a nonlinear particle filter (PF) to estimate the traffic stream density using CV data only. The proposed approaches are evaluated using empirical and simulated data, the former of which were collected along a signalized link in downtown Blacksburg, Virginia. Results indicate that density estimates produced by the linear KF approach are the most accurate. A sensitivity of the estimation approaches to various factors, including the level of market penetration (LMP) rate of CVs, the initial conditions, the number of particles in the PF approach, traffic demand levels, traffic signal control methods, and vehicle length, is presented. Providing accurate LMP estimates should improve the estimation accuracy of the vehicle counts. Therefore, in this research, a machine-learning model is developed to provide real-time estimates of the LMP values. Then, the developed filtering model is combined with the developed machine learning model (AKFNN) to improve the vehicle count estimation accuracy. Results show that the accuracy of the density estimate increases as the LMP increases. The KF is the least sensitive to the initial traffic density estimate, while the PF is the most sensitive to the initial traffic density estimate. The results also demonstrate that the proposed estimation approaches work better at higher demand levels given that more CVs exist for the same LMP scenario. For traffic signal control methods, the results demonstrate a higher estimation accuracy for fixed traffic signal timings at low traffic demand levels, while the estimation accuracy is better when the adaptive phase split optimizer is activated for high traffic demand levels. The report also investigates the sensitivity of the KF estimation approach to vehicle length, demonstrating that the presence of longer vehicles (e.g., trucks) in the traffic link reduces the estimation accuracy. In conclusion, the use of the linear KF approach is highly recommended in the application of traffic density estimation due to its simplicity and applicability in the field.

17. Key Words: Real-time estimation; probe vehicle; traffic density; neural network; connected vehicles; level of market penetration rate.	**18. Distribution Statement**		
19. Security Classif. (of this report) : Unclassified	**20. Security Classif. (of this page)** Unclassified	**21. No. of Pages** 61	**22. Price**

Contents

Table of Figures

List of Tables

Chapter 1. Development of a Kalman Filter Approach on an Isolated Intersection

1.1. Introduction

Real-time traffic estimation has received increased attention following the introduction of advanced technologies such as GPS units in vehicles. For instance, researchers have developed models to estimate the state of on-road traditional vehicles from known smart vehicle data. Smart vehicles are defined as vehicles that can exchange information, such as instantaneous speed, position, and acceleration, with other vehicles. This is generally referred to as vehicle-to-vehicle, or V2V, communication. These smart vehicles can also exchange information with road infrastructure, which is referred to as vehicle-to-infrastructure, or V2I, communication. However, there are currently a limited number of smart vehicles on the road and thus estimation becomes a crucial tool for obtaining a full picture of the traffic state.

This chapter employs real-time connected vehicle (CV) data to estimate one of the most important variables of signalized links: traffic density. Traffic density is defined as the number of vehicles per unit length along a given roadway segment (Roess, Prassas, and McShane 2011). Knowing the number of vehicles on a specific roadway segment is crucial to traffic management applications. These estimation outcomes are considered as an input to traffic signal controllers, leading to improved intersection performance as a result of reduced traffic delays, vehicle crashes, and vehicle emissions.

Previous studies have addressed this research problem using different traffic data sources to achieve the vehicle count estimation. Such sources have included traditional loop detectors (Vigos, Papageorgiou, and Wang 2008; Ghosh and Knapp 1978; Kurkjian et al. 1980; Bhouri et al. 1989), camera systems (Beucher, Blosseville, and Lenoir 1988), or fusion data (Anand, Vanajakshi, and Subramanian 2011; Anand, Ramadurai, and Vanajakshi 2014; van Erp, Knoop, and Hoogendoorn 2017; Qiu et al. 2010; Shahrbabaki et al. 2018), which combines two different sources of data, such as loop detectors with camera system, camera with GPS data, etc. The aforementioned detection techniques suffer from poor detection accuracy and are not cost-effective due to high installation fees and maintenance costs. More accurate data, such as data collected using the most recent technologies (i.e., CV data) are needed.

A loop detector can capture traffic state changes only around its location (stationary detection) and thus cannot address the research problem of estimating traffic density. Instead, two loop detectors, located at the entrance and exit of the traffic link, have generally been used to achieve the research goal after applying the traffic flow continuity equation. However, the noise in the extracted loop detector data leads to some errors in the estimation, an issue which is noted in the literature (Anand, Ramadurai, and Vanajakshi 2014; Vigos, Papageorgiou, and Wang 2008). To address the noise, the literature suggests using an additional source of data. (Vigos, Papageorgiou, and Wang 2008) used an additional loop detector in the middle of the tested link to reduce noise. However, the cost of implementing this model in the field is high, as it requires at least three loop detectors.

The Kalman filtering (KF) technique can be employed as a lower cost method (Kalman 1960) to estimate the number of vehicles. In a study by Anand et al., KF was combined with a video detection system and GPS data to estimate the traffic density (Anand, Ramadurai, and Vanajakshi 2014); the vehicle GPS data supplied the model with GPS-equipped vehicles' travel times. This approach is similar to the one presented in this chapter, but differs in two significant ways: 1) we only use CV data, and 2) we treat the estimation

interval time as a variable rather than keeping it constant (the estimation interval time was 60 s in (Anand, Ramadurai, and Vanajakshi 2014)). (van Erp, Knoop, and Hoogendoorn 2017) used data fusion to estimate the number of vehicles along an on-ramp link. They employed traffic count data from loop detectors and aggregated speeds from floating car data provided by Google, and set a 300-s fixed interval for updates.

Several studies have utilized KF to improve the estimation of various traffic variables, such as speed (Ye, Zhang, and Middleton 2006; Guo, Xia, and Smith 2009), travel time (Lee, Park, and Yun 2013; Chu, Oh, and Recker 2005), and traffic flow (Wang and Papageorgiou 2005). An unscented KF using single loop detectors (Ye, Zhang, and Middleton 2006) with a nonlinear state-space equation was able to improve speed estimates. Another study employed a linear KF technique to estimate speed, relying on the relationship between the flow-occupancy ratio and vehicle speed (Guo, Xia, and Smith 2009), yielding acceptable speed estimates for congested traffic conditions. A cumulative travel-time responsive real-time intersection control within a CVenvironment was also developed using the KF technique (Lee, Park, and Yun 2013). In that study, the authors recommended having levels of market penetration (LMP) of at least 30% in order to realize the algorithm's benefits. In summary, KF has proven to provide accurate estimates.

The proposed KF approach extends the state of the art in vehicle count estimates by making four major contributions:

1. The estimation approach relies solely on CV data. The approach was evaluated considering different CV LMPs ranging from 10% to 90% in increments of 10%.
2. The approach, unlike past applications, uses a variable estimation interval. Using a fixed estimation interval leads to inaccurate estimates, especially at low LMPs. Treating the estimation interval as a variable leads to an improved estimation technique. In this work, we defined the estimation interval as once exactly n CVs exit the link.
3. The chapter evaluates the impact of the signal control method (a fixed-time plan and an adaptive phase split optimizer) on the estimation accuracy.
4. The chapter investigates the sensitivity of the proposed estimation approach to vehicle length by introducing trucks into the traffic stream.

1.2. Estimation Approach

1.2.1. Define the Estimation Interval Time

This new approach improves the estimation accuracy, especially for low LMPs, as shown later in the Results section. The proposed approach defines the estimation interval time as the time when an exact number of CVs (n) exit the link. This ensures that sample of CVs remains the same in each estimation interval. For instance, if the LMP is low (e.g., 10%) and the estimation interval time is fixed and short (e.g., 20 s), there is no guarantee that CVs will be present on the link during the predefined short fixed-time interval, thus making the estimation inefficient and inaccurate. Accordingly, low LMPs require long intervals (e.g., 300 s). In contrast, links with high LMPs can use short fixed intervals (e.g., 20 s). However, the LMP is not a predefined factor and thus we cannot change the estimation interval time accordingly. A flexible approach is needed to overcome this issue and make the estimation more accurate and effective. The approach proposed in this work is a major contribution to traffic estimation, as it introduces the use of variable estimation periods to produce an efficient and convenient way of determining estimation interval periods. For the purpose of this chapter, the sample size is set to equal five CVs (n = 5) after testing different values (i.e., 1, 2, 3, 4, 5, 6, 7, 8, 9, and 10).

1.2.2. Estimation Approach Formulation

This section formulates an approach that estimates the total number of vehicles along signalized intersection links. The proposed estimation approach employs KF, using the state and measurement equations. The state equation utilizes the traffic flow continuity equation as defined in Equation (2), while the measurement equation is derived based on the hydrodynamic relation of traffic flow as defined in Equation (4). Equation (2) defines the number of vehicles by continuously adding the difference in the number of vehicles entering and exiting the link to the previously computed cumulative number of vehicles. This integral results in an accumulation of error that requires fixing, and thus requires the measurement equation.

$$N(t) = N(t - \Delta t) + \frac{\Delta t}{\rho}[q^{in}(t) - q^{out}(t)] \tag{2}$$

where $N(t)$ is the number of vehicles traversing the link at time t, $N(t - \Delta t)$ is the number of vehicles traversing the link in the previous time interval, and q^{in} and q^{out} are the CV flows entering and exiting the link between $(t - \Delta t)$ and t, respectively. ρ is the LMP of CVs, defined as the ratio of the number of CVs (N_{CV}) to the total number of vehicles (N_{total}), shown in Equation (3). For instance, if ρ is 0.1 and the number of CVs is 2, then the expected total number of vehicles is 20.

$$\rho = N_{CV}/N_{total} \tag{3}$$

Equation (4) describes the hydrodynamic relationship between the macroscopic traffic stream parameters (flow, density, and space-mean speed).

$$q = ku \tag{4}$$

where q is the traffic flow (vehicles per unit time), k is the traffic stream density (vehicles per unit distance), and u is the space-mean speed (distance per unit time) shown in Equation (5).

$$u = D/TT \tag{5}$$

where D is the link length and TT is the average vehicle travel time. Since CVs can share their instantaneous locations every Δt, the travel time of each CV can be computed for any road section. Thus, the CV travel time is used in the measurement equation, using Equations (4) and (5). The measurement equation can be written as shown in Equation (8):

$$TT(t) = D \times \frac{k(t)}{\bar{q}(t)} \tag{6}$$

$$TT(t) = \frac{1}{\bar{q}}[k(t) \times D] = \frac{1}{\bar{q}(t)}N(t) \tag{7}$$

$$TT(t) = H(t) \times N(t) \tag{8}$$

where $\bar{q}$ is the average traffic flow entering and exiting the link, and $H(t)$ is a transition vector that converts the vehicle counts to travel times and is the inverse of the average flow (i.e., the first term of Equation (7)), as shown in Equation (9).

$$H(t) = \frac{1}{\bar{q}(t)} = \frac{2 \times \rho}{q^{in}(t) + q^{out}(t)} \tag{9}$$

Note that the value of ρ in Equations (2) and (9) plays a major role in delivering accurate estimation outcomes. The proposed estimation approach (KF) equations are shown below:

$$\widehat{N}^{-}(t) = \widehat{N}^{+}(t - \Delta t) + \frac{\Delta t}{\rho}[q^{in}(t) - q^{out}(t)] \quad (10)$$

$$\widehat{TT}(t) = H\ (t)\ \times\ \widehat{N}^{-}(t) \quad (11)$$

$$\widehat{P}^{-}(t) = \widehat{P}^{+}(t-1) \quad (12)$$

$$G(t) = \hat{P}^{-}(t)H(t)^{T}\ [H(t)\hat{P}^{-}(t)\ H(t)^{T} + R]^{-1} \quad (13)$$

$$\widehat{N}^{+}(t) = \widehat{N}^{-}(t) + G(t)\ [TT(t) - \hat{TT}\ (t)] \quad (14)$$

$$\widehat{P}^{+}(t) = \widehat{P}^{-}(t) \times [1 - H\ (t)\ G\ (t)] \quad (15)$$

where $\widehat{N}^{-}$ is the a priori estimate of the vehicle counts calculated using the measurement prior to instant *t*, and $\widehat{P}^{-}$ is the a priori estimate of the covariance error at instant t. The Kalman gain (G) is computed using Equation (13). The R variable is the covariance error of the measurements. The posterior state estimate ($\widehat{N}^{+}$) and the posterior error covariance estimate ($\widehat{P}^{+}$) are updated as shown in Equations (14) and (15), considering the CVs' travel time measurements.

1.2.3. Define the LMP Rate (ρ)

This work tests the estimation approach using a predefined fixed ρ value over all the estimation intervals. For instance, the ρ value would be 10% for the entire evaluation if the scenario of 10% LMP is tested. The ρ values here are defined based on historic data. The ρ value is an important variable in the proposed estimation approach, as it scales up the CV observations to compute the total number of vehicles. The predefined ρ value is computed as the arithmetic mean of all ρ value observations. For instance, Figure 1.1 shows the actual ρ values (blue lines) versus the predefined ρ value (red line $\rho = 20\%$), which represents error in the approach estimating the ρ values. However, the KF can handle this error, as will be demonstrated later in the Results section.

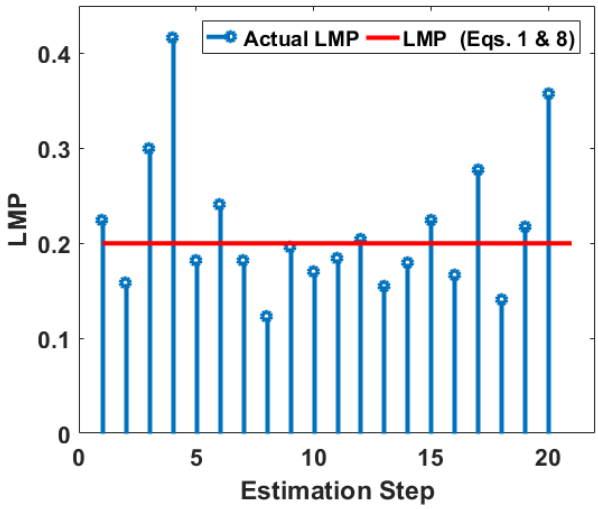

Figure 1.1 Actual LMP variations along the estimation steps.

1.3. Results and Discussion

This section presents the experimental setup (Section 1.3.1) and the experimental results (Section 1.3.2) of applying the proposed approach on an isolated intersection.

1.3.1. Experimental Setup

The proposed approach was tested on an intersection with four approaches comprised of three lanes each located in the heart of downtown Toronto (El-Tantawy and Abdulhai 2010), as shown in Figure 1.2. The traffic origin-destination (O-D) demand matrix, provided in Table 1.1, represents the highest total demand approaching the intersection during the afternoon rush hour (PM Peak) for the year 2005.

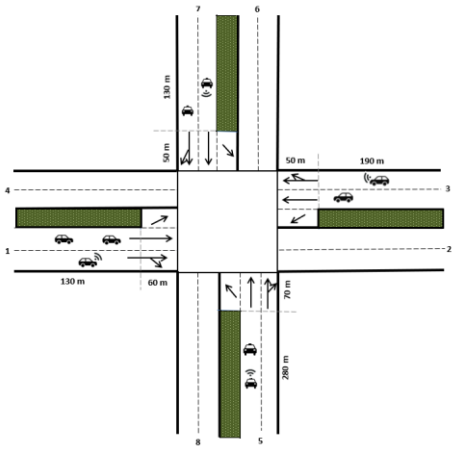

Figure 1.2 Simulated intersection.

Table 1.1 O-D demand matrix.

Zone #	2	4	6	8	Total
1	1,223	-	134	121	1,478
3	-	844	86	278	1,208
5	88	71	721	-	880
7	188	100	-	806	1,094
Total	1,499	1,015	941	1,205	4,660

The simulations were conducted using the following parameter values: speed at capacity = 60 (km/h), free-flow speed = 80 (km/h), jam density = 160 (veh/km/lane), saturation flow rate = 1,900 (veh/h/lane). The four-legged intersection's phasing scheme is shown in Figure 1.3. In this chapter, two signal operational approaches were conducted in order to achieve a more comprehensive analysis: a fixed-time traffic signal plan and an adaptive phase split optimizer (phase split). The fixed plan was computed using the Webster method (Daganzo and Daganzo 1997), with yellow and all-red times set at 3 s. The optimized effective green times for the four phases were 17 s, 13 s, 8 s, and 9 s. The phase split was optimized every 120 s. The optimization here allocates green time on the basis of the link's volume/saturation flow ratios according to the Canadian capacity guide and the highway capacity manual (Teply 1985).

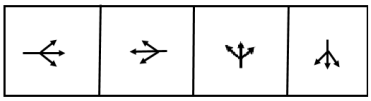

Figure 1.3 Four phasing scheme.

The accuracy of the proposed KF estimator was tested using the INTEGRATION microscopic traffic assignment and simulation software (Van Aerde and Rakha 2007) on an isolated intersection. The accuracy of the proposed estimation approach was evaluated based on the root mean square error (RMSE) and the relative root mean square error (RRMSE), as shown in Equations (16) and (17), respectively.

$$RMSE(veh) = \sqrt{\sum_{s=1}^{S} [\hat{N}^{+}(s) - N(s)]^2 / S} \quad (16)$$

$$RRMSE(\%) = 100 \sqrt{S \sum_{s=1}^{S} [\hat{N}^{+}(s) - N(s)]^2} / \sum_{s=1}^{S} N(S) \quad (17)$$

where $N(s)$ represents the actual vehicle count, $\hat{N}^{+}(s)$ represents the estimated vehicle count values, and S is the total number of estimations. The simulation starts with an initial estimate of ($\hat{N}^{+}(0) = 5$ veh) as in (Vigos, Papageorgiou, and Wang 2008), an initial posterior estimate error of ($\hat{P}^{+}(0) = 5$), and measurement error covariance of ($R = 5$).

1.3.2. Experimental Results

This section compares the performance of the proposed estimation approach using two estimation interval times: a fixed estimation interval (i.e., 60 and 120 s) and the proposed variable estimation interval approach. Recall that the variable estimation interval time is defined when a certain number of CVs (e.g. 5 veh) reach the end of the link (i.e., the traffic signal stop bar; Section 1.3.2.1). Section 1.3.2.2 describes the effect of the signal timing plan on the estimation results. Section 1.3.2.3 describes the impact of heavy trucks on the estimation accuracy.

1.3.2.1. Variable vs. Fixed Estimation Time Interval

Previous research has considered fixed estimation intervals (e.g., 30 s). This is an appropriate approach if data from all vehicles are available and can be used (LMP of 100%). However, this condition is impossible to obtain when CV data are used. Consequently, the use of variable interval time steps is crucial for obtaining high estimation accuracy and avoiding the absence of CV data in any estimation interval.

This section illustrates the benefits of using variable time steps as opposed to a constant value. Table *1.2* presents the estimation efficiency using fixed and variable time steps in the eastbound (EB) approach. The fixed intervals are considered to be the same as traffic cycle lengths (i.e., 60 and 120 s). Moreover, different LMPs were considered to provide a comprehensive comparison. It is clear that the proposed strategy of using variable time steps significantly improves the estimation accuracy results and always ensures that the same amount of information is present for every time step (five CVs). It is clear that the estimation approach with fixed intervals is not applicable, as the scenario for 10% LMP shows; this is due to the absence of observed CVs in most time intervals. Longer estimation intervals are required when LMPs are low (e.g., 200 s) to ensure that some CVs are on the link, and thus available information is employed in the KF. In contrast, shorter estimation intervals are utilized when LMPs are high (e.g., 30 s). The strategy proposed herein ensures flexibility of the estimation interval times.

Table 1.2 EB RRMSE of fixed and variable estimation time interval.

LMP (%)	**RRMSE (%)**		
	Fixed ($\Delta t = 60$ s)	Fixed ($\Delta t = 120$ s)	Proposed Approach
10	Not a Number	48	41
20	45	42	39
30	44	39	35
40	41	36	31
50	39	35	27
60	37	36	25
70	36	34	23
80	34	34	21
90	34	33	20

1.3.2.2. Fixed vs. Optimized Green Traffic Signal Timing

This section studies the impact of allocated green signal timing on the estimation accuracy using a fixed plan (green times for all traffic signal phases are predefined and remain fixed) and an adaptive phase split optimizer. The total number of vehicles along the tested links were estimated considering different LMPs (10% to 90%). A Monte Carlo simulation was conducted to create 100 random CV samples from the entire data set for each scenario. This section presents the estimation results of the intersection links: EB (Table 1.3), westbound (WB, Table *1.4*), northbound (NB, Table *1.5*), and southbound (SB, Table *1.6*).

The results show that the algorithm produces more accurate estimations for the fixed-time plan for the minor approaches (NB, SB). In contrast, the estimation accuracy improves with optimization for the high-demand approaches (EB and WB). The phase split optimizer positively impacts approaches with high traffic demand levels, as more green times are allocated, and thus the estimation polling interval is shorter (more vehicles are expected to traverse the intersection). In addition, the results show that the estimation accuracy increases as the LMP increases, as the CVs supply more data. For example, if the entire data set contains 1,000 vehicles (CVs and traditional), and the LMP on the link is equal to 10%, then the number of CVs is

100. On the other hand, if the LMP is equal to 90%, the number of CVs is 900. In conclusion, having more information significantly improves estimation accuracy.

Table 1.3 EB RRMSE and RMSE using fixed and phase split plans.

LMP (%)	**Fixed Plan**		**Phase Split**	
	RRMSE (%)	RMSE (veh)	RRMSE (%)	RMSE (veh)
10	41	4.4	39	4.5
20	39	4.1	37	4.2
30	35	3.8	33	3.9
40	31	3.3	31	3.5
50	27	3.0	27	3.1
60	25	2.7	24	2.8
70	23	2.4	21	2.4
80	21	2.2	18	2.1
90	20	2.2	15	1.7

Table 1.4 WB RRMSE and RMSE using fixed and phase split plans.

LMP (%)	**Fixed Plan**		**Phase Split**	
	RRMSE (%)	RMSE (veh)	RRMSE (%)	RMSE (veh)
10	48	4.5	39	4.6
20	44	4.1	36	4.2
30	40	3.7	33	4.0
40	38	3.5	31	3.7
50	38	3.5	28	3.4
60	37	3.3	26	3.1
70	37	3.3	24	2.8
80	33	3.0	22	2.6
90	27	2.5	21	2.6

Table 1.5 NB RRMSE and RMSE using fixed and phase split plans.

LMP (%)	**Fixed Plan**		**Phase Split**	
	RRMSE (%)	RMSE (veh)	RRMSE (%)	RMSE (veh)
10	25	4.4	36	5.2
20	25	4.4	33	4.6
30	23	4.1	29	4.2
40	23	3.9	29	4.1
50	22	3.7	28	3.9
60	20	3.5	26	3.7
70	19	3.3	25	3.5
80	19	3.3	23	3.3
90	17	3.0	23	3.3

Table 1.6 SB RRMSE and RMSE for fixed and phase split plans.

LMP (%)	Fixed Plan		Phase Split	
	RRMSE (%)	RMSE (veh)	RRMSE (%)	RMSE (veh)
10	29	3.8	45	4.6
20	29	3.7	43	4.4
30	26	3.3	36	3.8
40	25	3.2	32	3.3
50	22	2.8	29	3.0
60	20	2.6	26	2.9
70	19	2.5	24	2.5
80	19	2.4	22	2.2
90	18	2.3	22	2.2

The proposed approach addresses the research goal appropriately, producing reasonable error values. Vigos et al. considered their model with up to a 27.5% RRMSE using three loop detector measurements (Vigos, Papageorgiou, and Wang 2008). Our approach used no loop detectors and low LMPs, and still produced RRMSE values close to Vigos et al.'s model, which used an LMP of 100% and the three aforementioned loop detectors.

1.3.2.3. Impact of Heavy Trucks

This section investigates the sensitivity of the proposed estimation approach to vehicle length. Trucks with 4 times the normal vehicle length were introduced to the EB base scenario on all movements. Two different percentages were used to define the number of trucks on the tested links: 5% and 10% of the entire data set. Table *1.7* illustrates the impact of trucks on estimation accuracy. In the presence of trucks, the maximum link accommodation was less compared to the base scenario. As these results show, trucks reduce estimation accuracy by increasing bias in our approach. This finding is in line with Vigos et al.'s conclusion (Vigos, Papageorgiou, and Wang 2008).

Table 1.7 RRMSE in scenarios with no trucks, 5%, and 10% trucks.

LMP (%)	Base Scenario	5% Trucks	10% Trucks
10	41	43	49
20	39	42	46
30	35	39	41
40	31	34	36
50	27	29	31
60	25	26	27
70	23	24	24
80	21	25	22
90	20	25	21

1.4. Summary and Conclusions

This chapter proposes a novel approach for estimating the number of vehicles approaching a traffic signal using CV data only. The approach uses a variable estimation interval rather than the traditional fixed interval. Specifically, the duration of the interval is dynamically computed when a predefined sample size (n) exits the link. This improves the estimation accuracy, especially for low LMPs, and makes the proposed estimation approach flexible. The estimation approach uses the known KF technique to achieve the research goal. The proposed KF estimator was employed to test the model's accuracy on signalized multi-lane roads. The results showed that the proposed KF addressed the research goal by producing reasonable errors, even

at low LMPs. The results indicated, as would be expected, that estimation errors decrease as the LMP increases. In addition, the approach was evaluated considering two traffic signal timing scenarios: a fixed-time plan and an adaptive phase split optimizer. The results demonstrated that the approach works better for the fixed plan at lower traffic demand levels. Alternatively, the approach works better for the adaptive traffic signal controller for high approach traffic demand levels. This was a result of extending the green times for the higher traffic demand approaches, which produced shorter estimation intervals, as n CVs traversed the link in shorter time periods. Finally, the chapter investigated the sensitivity of the KF's accuracy when adding some trucks to the traffic flow. Specifically, the chapter tested for 5% and 10% trucks of the original demand. The estimation accuracy was found to decrease as the percentage of trucks increased.

Chapter 2. Development of Adaptive Kalman and Neural Kalman Filtering Approaches

2.1. Introduction

Real-time traffic state estimates have grown increasingly important following the introduction of recent advanced technologies such as CVs. CVs aim to improve road safety by potentially reducing human errors, mitigating traffic congestion levels by offering alternative routes, and reducing on-road emissions and fuel consumption (Zmud et al. 2017). Nowadays, conducting research with limited probe vehicle data (e.g., CVs) is a challenge, especially when no additional data sources are provided. Hence, past research has utilized CV data in conjunction with existing detection systems to enhance proposed traffic models, despite the limitation that fixed detection techniques (e.g., loop detectors) always have some noise in their data (Anand, Ramadurai, and Vanajakshi 2014; Anand, Vanajakshi, and Subramanian 2011; Badillo et al. 2012).

A CV is defined as a vehicle that provides real-time information, such as instantaneous position and speed. Several benefits of using CV data have been recognized; for example, the high quality of the data compared with existing data sources (e.g., cameras and loop detectors), and the ability for data to be collected at any location inside the network, thus offering a clear picture about traffic behavior at any time. Therefore, transportation agencies are putting effort into facilitating the use of CV data.

Limited studies have used CV-only data to estimate the state of on-road traditional vehicles (Aljamal, Abdelghaffar, and Rakha 2019b), such as traffic travel time, traffic density, traffic speed, and traffic volume. The real-time estimation of traffic density is important to achieving better traffic operations management in urban areas. This chapter aims to estimate the total number of vehicles on signalized links using only CV data. The estimate outcomes can be provided to traffic signal controllers to optimally determine the allocation of green time for each traffic signal phase (Abdelghaffar, Yang, and Rakha 2017; Abdelghaffar and Rakha 2019), leading to better intersection performance measures such as intersection delays and vehicle crashes (Rakha and Van Aerde 1995; Abdelghaffar, Yang, and Rakha 2018). One concern with using CVs is measuring their LMP. The LMP is defined as the ratio of the total number of CVs to the total number of vehicles. Providing accurate LMP estimates improves the estimation accuracy of the vehicle counts (Aljamal, Abdelghaffar, and Rakha 2019b, 2020b). Therefore, in this chapter, a machine-learning technique is developed to provide reliable LMP estimates.

2.2. Related Work

Different statistical tools have been used to estimate the total number of vehicles on arterial roads and freeways, such as the KF (Kalman 1960), Bayesian statistics (Press and Shigemasu 1989), and particle filter (Del Moral 1996) (Aljamal, Abdelghaffar, and Rakha 2020a) approaches. The literature shows the benefits of using the KF technique in addressing different aspects of the traffic estimation problem. The KF has been used to estimate the traffic travel time, traffic speed, and traffic density. Different detection techniques have been employed to estimate the number of vehicles, such as loop detectors, camera systems, and probe data. Two loop detectors, one at the entrance and the other at the exit of the link, are utilized to measure the total number of arrivals and departures, then the number of vehicles is simply obtained by applying the flow continuity equation (Roess, Prassas, and McShane 2011). In one study, a robust KF model with at least three loop detectors on the tested link was employed to estimate the number of vehicles on the link in (Vigos, Papageorgiou, and Wang 2008). The study derived the KF state equation from the flow continuity equation, while the measurement equation was derived from the relationship of the detector time-occupancy

and space-occupancy; however, the cost of implementing such an algorithm in the field is high given the number of sensors needed. Another study employed the KF to estimate the number of vehicles on multi-section freeways. The state equation was derived from the flow continuity equation, while the measurement equation was derived from the hydrodynamic relationship between traffic speed and density (Gazis and Liu 2003). Loop detectors were used in addition to speed sensors in the middle of the tested section. However, the proposed algorithm is hard to employ in the field due to the high cost of implementation. A video record, another detection technique, was used to estimate the traffic density for signalized links (Ajitha, Vanajakshi, and Subramanian 2013). In that study, the authors used the space-mean speed rather than the traffic flow in the state equation due to high errors accompanied with sensor failures. Their argument takes into account that the space-mean speed is taken as an average quantity while the traffic flow is a cumulative quantity. They also demonstrated the importance of having knowledge about the system noise characteristics to improve the performance of the KF model. Consequently, an adaptive Kalman filter (AKF) was developed to enable real-time estimates of statistical parameters of the system noise rather than using predefined values for the entire simulation (as assumed in the traditional KF approach).

As illustrated in the literature, stationary sensors, such as loop detectors and camera systems, suffer from poor detection accuracy and have high installation and maintenance costs. Advanced detection techniques such as CV data have proven to be more accurate without the need to install additional hardware. Consequently, recent studies have developed several traffic estimation models using fusion data (combination of two different data sources) to estimate the number of vehicles with the aim of achieving better accuracy than using only one source of data. In many of the works using fusion data, the KF technique was employed for estimating traffic density. One study achieved accurate estimated traffic density results using the traffic flow values measured from a video detection system and the travel time obtained from vehicles equipped with GPS devices (Anand, Vanajakshi, and Subramanian 2011). The proposed estimation approach in this study differs in two significant ways from the proposed AKF approach, namely only CV data are used with a variable time interval rather than a fixed value (the updating time interval was 1 minute in (Anand, Vanajakshi, and Subramanian 2011)), and the proposed estimation approach uses the AKF to allow for real-time estimates of statistical parameters of the state and measurement noise.

Reviewing the literature, the KF model has proven its ability to address estimation research problems for different traffic applications. However, it is hard to implement in real-world applications due to the difficulty of estimating the statistical characteristics of the system noise (mean and variance). Consequently, researchers have developed the AKF to solve this issue and make field implementation possible. Chu et al. proposed an AKF approach to estimate freeway travel time using both loop detectors and CV data (Chu, Oh, and Recker 2005). They presented the estimation method for noise statistic parameters that was proposed in (Myers and Tapley 1976), which is known for its simplicity in handling errors and its fast processing time. Hence, in this chapter, the estimation of the statistical parameters uses the same estimation procedure as in Chu et al.'s study. It should be noted that the main difference between the proposed estimation approach and Chu et al.'s approach is that our approach uses only CV data.

In a recent study, the KF approach was proposed to estimate the number of vehicles on signalized links using only CV data (Aljamal, Abdelghaffar, and Rakha 2019b). The KF state equation was based on the traffic flow continuity equation and thus one value of CV LMP (ρ), for the entire link, was used to scale up the CV measurements to reflect the total flow in the second term of the flow continuity equation as presented in Equation (18). It was found that using two LMP values (at the entrance and the exit of the link) produces

more accurate vehicle count estimates, especially when dealing with low LMPs, as described later in Section 2.4. In Equation (18), $N(t)$ is the number of vehicles traversing the link at time (t), Δt is the variable duration of the updating time interval, $N(t-\Delta t)$ is the number of vehicles traversing the link in the previous interval, q^{in} and q^{out} are the CV flows entering and exiting the link between $(t-\Delta t)$ and (t), respectively, and ρ is the LMP of CVs.

$$N(t) = N(t-\Delta t) + \frac{\Delta t}{\rho}[q^{in}(t) - q^{out}(t)] \quad (18)$$

Machine learning has proven its ability to provide accurate estimates for different traffic characteristics (Fulari, Vanajakshi, and Subramanian 2017; Antoniou and Koutsopoulos 2006; Khan, Dey, and Chowdhury 2017; Wassantachat et al. 2009; Jahangiri, Rakha, and Dingus 2015; Sekuła et al. 2018). Traffic speed and density have been estimated using an artificial neural network (ANN) model (Fulari, Vanajakshi, and Subramanian 2017). Video and Bluetooth data were used to build the ANN model. The traffic flow data were manually extracted from the video records, while the speed data were constructed from the collected Bluetooth travel time data. The ANN model is able to address the research problem if a good quantity of training data is accessible. Another study conducted several machine learning techniques such as *k*-means clustering, *k*-nearest neighbor classification, and locally weighted regression to estimate traffic speed (Antoniou and Koutsopoulos 2006) using archived data of speeds, counts, and densities. They found that machine learning models can improve the accuracy of speed estimation. Khan et al. (Khan, Dey, and Chowdhury 2017) used artificial intelligence to classify the level of service in a freeway segment based on traffic density values. They used loop detectors and CV data to develop support vector machine and *k*-nearest neighbor classification. Results indicated higher accuracy from the support vector machine algorithm than the *k*-nearest neighbor classification algorithm. Estimating hourly traffic volumes between sensors was addressed using an ANN model in the Maryland highway network (Sekuła et al. 2018), deploying both CVs and automatic traffic recording station data to construct the ANN model. A comparison was also made between linear regression, *k*-nearest neighbor, support vector machine with linear kernel, random forest, and ANN models, concluding that the ANN model performed the best. The proposed approach produced 24% more accurate estimates than current volume profiles.

In this chapter, an AKF approach is applied to estimate real-time vehicle counts along signalized links using only CV data. The study then considers the recommendation of Aljamal et al.'s study (Aljamal, Abdelghaffar, and Rakha 2020b) by using two LMP values at the entrance and the exit of the tested link. To achieve this task, an ANN approach was developed to provide real-time estimates of the LMP values to improve the accuracy of the proposed AKF approach. After that, the chapter develops the new AKFNN approach after combining the AKF with the developed ANN approach. This chapter extends the state of the art in vehicle count estimates by making four major contributions:

1. This chapter tests the proposed AKF approach using only CV data. The approach was evaluated considering different CV LMPs ranging from 10% to 90% in increments of 10%.
2. The chapter develops an ANN approach to estimate the LMP of CVs at the exit of the link to reflect the total vehicle departures.
3. The chapter tests the developed AKFNN approach by using a fusion of CV and single loop detector data. A comparison between the traditional KF, AKF, and AKFNN approaches is presented.

4. The chapter examines the impact of the initial conditions on the AKF estimation approach. Three initial condition parameters are tested: the initial vehicle count estimate, the initial mean estimate of the state noise errors, and the a priori initial covariance of the state system.

This chapter is organized as follows. Section 2.3 describes the development of the simulation data. Section 2.4 describes the development of the KF, AKF, and AKFNN estimation approaches. Section 2.5 discusses the results of the estimation approaches. Section 2.6 provides the conclusions of the chapter.

2.3. Development of Simulation Data

This chapter relies on the INTEGRATION traffic simulation model (Van Aerde and Rakha 2007) to validate and test the accuracy of the proposed approaches. The INTEGRATION software has been extensively validated and demonstrated to replicate empirical observations (Dion, Rakha, and Kang 2004; Rakha, Kang, and Dion 2001; Chamberlayne, Rakha, and Bish 2012; Rakha, Pasumarthy, and Adjerid 2004; Aljamal et al. 2018). Specifically, INTEGRATION was used to create synthetic data for conditions not observed in the field to quantify the sensitivity of the proposed method to the link length and traffic demand level. The selected tested link is located in downtown Blacksburg, Virginia, with an approximate length of 102 m based on ArcGis software, and connects two signalized intersections. The link characteristics were calibrated to local conditions using typical values, which included a free-flow speed of 40 (km/h), a speed at capacity of 32 (km/h), a jam density of 160 (veh/km/lane), and a base saturation flow rate of 2,100 (veh/h/lane), which resulted in a roadway capacity of 700 (veh/h) given the cycle length and green times of the traffic signal. The traffic signal cycle length is 75 s and it has four phases with the following displayed green times: 5, 25, 5, and 28 s. The tested link here is assigned with a displayed green time of 25 s. These values were consistent with what was coded in the field.

The INTEGRATION simulation model was used to ease the generation of CV data as real CV data are not easy to access. For each LMP, a total of 50 scenarios were generated with different random seeds as conducted in (Khan, Dey, and Chowdhury 2017). Forty-nine scenarios were used to train and validate the proposed ANN approach, and scenario number 50 was considered the testing data set. The INTEGRATION model generates a "time-space" file which provides some information about the CVs during their trips for every second. The time-space file records the instantaneous position, speed, and spacing for each CV. In addition to that, a loop detector is installed at the entrance of the tested link to create a detector output file which provides some data about the simulation behavior such as speed, traffic volume, and occupancy at the detection location.

2.4. Estimation Approaches

This section first summarizes some crucial points regarding estimating the vehicle count as discussed in Chapter 3. In addition, this section describes the proposed AKF estimation approach for estimating the vehicle count along signalized link approaches, and demonstrates the difference of the state-of-the-art KF approach in Aljamal, Abdelghaffar, and Rakha (2019b) and the new proposed AKF approach. Finally, an ANN approach is developed to provide estimates of the CV LMPs to be used in the proposed AKF approach equations to attain higher accuracy. Two vehicle count estimation approaches are described in this section: (1) the AKF, which uses only CV data; and (2) the AKFNN, which fuses CV and single loop detector data. The single loop detector data were mainly used to develop the ANN approach.

2.4.1. Summary of the Developed KF Approach

In a previous study (Aljamal, Abdelghaffar, and Rakha 2019b), the authors developed a KF approach to produce reliable vehicle count estimates using only CV data. In that study, the authors introduced a novel variable estimation time interval as opposed to the traditional fixed time interval. The estimation time interval was defined as the time when exactly n CVs traversed the tested link. It was proven that the variable time interval, compared to a fixed time interval (e.g., 20 s), led to improved estimation accuracy. An illustrative example shows the benefits of using the variable time interval. If the approach's LMP is 10%, the number of CVs will obviously be low. If we treat the problem using a fixed estimation interval, then the probability of observing zero CVs within an interval will be high for short estimation time intervals, making the estimation inefficient and inaccurate. Accordingly, low LMPs require long intervals (e.g., 300 s) to ensure that at least one CV is on the approach. In contrast, approaches with high LMPs can use short estimation intervals (e.g., 20 s). Consequently, treating the estimation time interval as a variable produces an efficient and convenient way of determining the duration of the estimation period.

One concern about the KF approach is the use of predefined fixed values of the mean and variance of the KF state and measurement errors. Applying the KF in real-world problems is limited since the statistical parameters are assumed to be known (Chu, Oh, and Recker 2005). The mean and variance entities are known as variable rather than fixed values. To produce a flexible model, this chapter employs the AKF to provide real-time estimates of the statistical parameters of the KF state and measurement errors as described in the following section.

2.4.2. Adaptive Kalman Filter (AKF)

The traditional KF is utilized with predefined error values of the state and measurement noise; these error values remain constant for the entire simulation. However, these values are hard to obtain in the field and they are always changing with time. Hence, an AKF was developed to overcome this issue and to dynamically estimate the error values in the state and measurement estimates. The AKF is comprised of two equations: (a) state equation and (b) measurement equation. The state equation is derived from the traffic flow continuity equation as defined in Equation (19). The state equation computes the number of vehicles by continuously adding the difference in the number of vehicles entering and exiting the section to the previously computed cumulative number of vehicles traveling along the section. This integral results in an accumulation error which requires fixing, and thus the measurement equation is needed. In Equation (19), the ρ value can be observed from historical data.

$$N(t) = N(t - \Delta t) + \frac{\Delta t}{\rho}[q^{in}(t) - q^{out}(t)] \quad (19)$$

The state equation produces accurate results if the scaled traffic flows (q^{in}/ρ_{in} and q^{out}/ρ_{out}) are accurate, as shown in Section 2.5. The total counts can be extracted from traditional loop detectors or video detection systems. We should note here that the ρ value in Equation (19) plays a major role in delivering accurate outcomes. ρ is defined as the ratio of the number of CVs (N_{CV}) to the total number of vehicles (N_{total}), as shown in Equation (20). For instance, if ρ equals 0.1, and the number of CVs is 5, then the expected total number of vehicles is 50.

$$\rho = N_{CV}/N_{total} \quad (20)$$

Equation (21) describes the hydrodynamic relationship between the macroscopic traffic stream parameters (flow, density, and space-mean speed),

$$q = ku_s \quad (21)$$

where q is the traffic flow (vehicles per unit time), k is the traffic stream density (vehicles per unit distance), and u_s is the space-mean speed (distance per unit time). The u_s can be represented as shown in Equation (22),

$$u_s = D/TT \tag{22}$$

where D is the link length and TT is the average vehicle travel time. Since CVs can share their instantaneous locations every Δt, the travel time of each CV can be computed for any road section. Thus, the CV travel time is used in the measurement equation, using Equations (21) and (22). The measurement equation can be written as shown in Equation (25):

$$TT(t) = D \times \frac{k(t)}{\bar{q}(t)} \tag{23}$$

$$TT(t) = \frac{1}{\bar{q}}[k(t) \times D] = \frac{1}{\bar{q}(t)} N(t) \tag{24}$$

$$TT(t) = H(t) \times N(t) \tag{25}$$

where $\bar{q}$ is the average traffic flow entering and exiting the link, and $H(t)$ is a transition vector that converts the vehicle counts to travel times, and is the inverse of the average flow (i.e., the first term of Equation (24)), as shown in Equation (26).

$$H(t) = \frac{1}{\bar{q}(t)} = \frac{2\times\rho}{q^{in}(t)+q^{out}(t)} \tag{26}$$

The system state and measurement equations can be written as in Equations (27) and (28), considering the error (noise). The term $u(t)$ is the given inputs for the system. The vector $H(t)$ is used to convert the vehicle counts to travel times. The vector $w(t-\Delta t)$ is the state noise and is assumed to be Gaussian noise with the mean of $m(t)$ and variance of $M(t)$. The measurement noise $v(t)$ is assumed to be Gaussian noise with the mean of $r(t)$ and variance of $R(t)$.

$$\text{State Equation:} \quad N(t) = N(t-\Delta t) + u(t) + w(t-\Delta t) \tag{27}$$

$$u(t) = \frac{\Delta t}{\rho}[q^{in}(t) - q^{out}(t)]$$

$$\text{Measurement Equation: } TT(t) = H(t) \times N(t) + v(t) \tag{28}$$

$$H(t) = \frac{1}{\bar{q}(t)} = \frac{2\times\rho}{q^{in}(t)+q^{out}(t)}$$

The proposed AKF estimation approach can be solved using the following equations:

$$\widehat{N}^{-}(t) = \widehat{N}^{+}(t-\Delta t) + u(t) + m(t-\Delta t) \tag{29}$$

$$\widehat{P}^{-}(t) = \widehat{P}^{+}(t-\Delta t) + M(t-\Delta t) \tag{30}$$

$$G(t) = \hat{P}^{-}(t)H(t)^{T}\,[H(t)\hat{P}^{-}(t)\,H(t)^{T} + R(t)]^{-1} \tag{31}$$

$$\widehat{N}^{+}(t) = \widehat{N}^{-}(t) + G(t)\,[TT(t) - H(t)\widehat{N}^{-}(t) - r(t)] \tag{32}$$

$$\widehat{P}^{+}(t) = \widehat{P}^{-}(t) \times [1 - H(t)\,G(t)] \tag{33}$$

where $\widehat{N}^-$ is the a priori estimate of the vehicle counts calculated using the measurement prior to instant *t*, and $\widehat{P}^-$ is the a priori estimate of the covariance error at instant t. The Kalman gain (G) is demonstrated in Equation (31). The posterior state estimate ($\widehat{N}^+$) and the posterior error covariance estimate ($\widehat{P}^+$) are updated as shown in Equations (32) and (33), considering the CV travel time measurements. In the next section, the estimation steps for the noise statistical parameters (m, M, r, R) are described.

2.4.2.1. Online Estimation of Noise Statistics

An online estimate is conducted to optimally find the errors in the state and the measurement variables to make the KF more efficient and applicable in real-world applications. As pointed out in the literature, the traditional KF assumes predefined errors in the system, which is not the case in real applications. A set of unknown noise statistical parameters, (m, M, r, R), needs to be estimated at every estimation step. The online estimate procedure follows the same procedure presented in Chu, Oh, and Recker (2005).

The mean (m) and variance (M) of the state noise are shown in Equations (34) and (35), respectively.

$$m = \frac{1}{n}\sum_{t=1}^{n} \; m(t), \quad \text{where} \;\; m(t) = \widehat{N}^+(t) - \widehat{N}^+(t - \Delta t) - u(t) \tag{34}$$

$$M = \frac{1}{n-1}\sum_{t=1}^{n} \; [(m(t) - m).(m(t) - m)^T - (\frac{n-1}{n})\hat{P}^+(t - \Delta t) - \hat{P}^+(t)] \tag{35}$$

where $m(t)$ is the state noise at time t, the first term of Equation (35) is the covariance of *w* at time t, and *n* is the number of state noise samples.

The mean (r) and variance (R) of the measurement noise are shown in Equations (36) and (37), respectively.

$$r = \frac{1}{n}\sum_{t=1}^{n} r(t), \quad \text{where} \; r(t) = TT(t) - H(t)\,\widehat{N}^-(t) \tag{36}$$

$$R = \frac{1}{n-1}\sum_{t=1}^{n} \; [(r(t) - r).(r(t) - r)^T - (\frac{n-1}{n})H(t)\hat{P}^-(t)H^T(t)] \tag{37}$$

where $R(t)$ is the observation noise at time t. The first term of Equation (37) is the covariance of *v* at time t, and *n* is the number of measurement noise samples. As a summary, the KF and AKF approaches use the same equations except for the fact that the AKF estimates the statistical parameters of the noise for every estimation step using Equations (34) to (37).

As found in Chapter 1, providing the system equations real-time estimates of ρ_{in} and ρ_{out} should improve the estimation accuracy. In this chapter, a single loop detector was installed at the entrance of the tested link to produce real-time estimates of ρ_{in}. In contrast, in the next section, an ANN is developed to obtain real-time estimates for the ρ_{out} values.

2.4.3. Artificial Neural Network

ANN is a machine learning technique that aims to recognize relationships between vast amounts of data by employing a certain number of neurons in every single hidden layer to achieve better accuracy (Haykin 2007). The network consists of three main layers: the input layer, the hidden layer, and the output layer. This section takes into account the recommendation of using two market penetration rates (at the entrance and exit of the link) rather than one market penetration rate along the tested link in the KF equations (Aljamal, Abdelghaffar, and Rakha 2019b). Accordingly, the state equation and the H vector in the

measurement equation are revised as presented in Equations (38) and (39). ρ_{in} and ρ_{out} are the CV LMP at the entrance and the exit of the link, respectively.

$$N(t) = N(t - \Delta t) + \Delta t[\frac{q^{in}(t)}{\rho_{in}(t)} - \frac{q^{out}(t)}{\rho_{out}(t)}] \quad (38)$$

$$H(t) = \frac{1}{\bar{q}(t)} = \frac{2}{\frac{q^{in}(t)}{\rho_{in}(t)} + \frac{q^{out}(t)}{\rho_{out}(t)}} \quad (39)$$

A single loop detector was installed at the entrance of the link to measure ρ_{in} and also to use as an input to the ANN approach. Accordingly, this chapter develops an ANN approach to estimate ρ_{out}. The tested link is shown in Figure 2.1. The next section describes the selected inputs (features) and the output variables of the ANN approach.

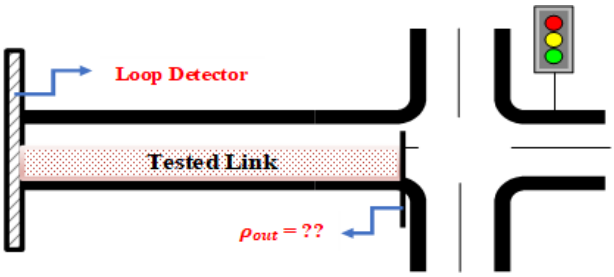

Figure 2.1 Tested link.

2.4.3.1. Characteristics of the ANN: Input and Output Variables

Previous research has used different features to build machine learning models (Fulari, Vanajakshi, and Subramanian 2017; Antoniou and Koutsopoulos 2006; Khan, Dey, and Chowdhury 2017; Wassantachat et al. 2009). Fusing video and Bluetooth data was used to estimate traffic density and speed. The traffic flow was manually extracted from the video records, while the speed data were constructed from the collected Bluetooth travel time data (Fulari, Vanajakshi, and Subramanian 2017). Another study relied on archived data of traffic speeds, counts, and density to estimate traffic speed (Antoniou and Koutsopoulos 2006). Distance headway, number of stops, and speed data were identified as useful features to achieve accurate density estimates (Khan, Dey, and Chowdhury 2017). They employed loop detectors and CV data. In a recent study, Sekula et al. (Sekuła et al. 2018) used probe and automatic traffic recording station data to extract the features of the ANN model. The selected features were the (1) speed of the CVs; (2) weather data such as temperature, visibility, precipitation, and weather status; (3) infrastructure data (speed limits, number of lanes, class of the road, and type of the road); (4) temporal data such as the day of the week; and (5) volume profiles based on historical data. The literature showed that traffic speed is always used as a model feature, especially when CV data are used. In contrast, traffic flow is always a feature when stationary sensors (e.g., loop detector) are used.

This research utilizes a fusion of CV and single loop detector data to produce the ANN features. The single loop detector was installed at the entrance of the link, and thus ρ_{in} can be computed directly using Equation (20). The ρ_{out} variable is calculated from the ANN (the ANN output). Seven possible inputs (features) were considered in the ANN, as defined in Table 2.1. Conducting a feature selection technique to validate the importance of each feature for the ANN approach, the number of the model features was dropped to five.

It should be noted that the selected inputs can be easily extracted when CVs are on the link. ρ_{out} can be expressed as a function of the selected inputs, as presented in Equation (40).

$$\rho_{out} = f(A_t, A_p, u_s, S_1, S_2) \tag{40}$$

The ρ_{out} values vary between 0 and 1; a 0 value means that no CVs were observed at the exit of the link, while the value of 1 means that the D_{CV} value is the same as the D_t. The selected inputs must be relevant to the model output ρ_{out} to allow the ANN model to build a strong relationship between the model inputs and outputs and therefore produce high estimation accuracy. For instance, in our case, the ρ_{out} value decreases as A_t and A_{CV} increase. For instance, a high value of A_t means that the link is more congested and thus the number of departures (D_t) is expected to be high. The ρ_{out} value also decreases with increasing speed (S_1, S_2, and u_s). The speed is an indicator of the congestion level of the link; for instance, if the speed is low, then more vehicles are expected to be on the link, leading to higher values of D_t.

Table 2.1 Definition of the ANN approach inputs.

Input Symbol	Definition	Unit
A_t	Total number of arrivals obtained from the single-loop detector	veh
A_{CV}	Total number of CV arrivals	veh
D_{CV}	Total number of CV departures	veh
S_1	Average speed for CVs at link entrance	km/hr
S_2	Average speed for CVs at link exit	km/hr
u_s	Space-mean speed for CVs	km/hr
u_t	Time-mean speed for CVs	km/hr

A single hidden layer with one neuron, with a transfer function of hyperbolic tangent sigmoid, was used to build the ANN model as shown in Figure *2.2*. The Levenberg-Marquardt (LM) optimization has been proven in the literature to outperform the gradient decent and conjugate gradient methods for medium-sized problems (Roweis 1996). Furthermore, the LM is considered the fastest back-propagation algorithm and thus was implemented in the proposed approach. The weights and biases of the developed ANN approach are described below. w_1 depicts the weights between the input layer and the hidden layer, while w_2 represents the weight between the hidden layer and the output layer. $b1$ and $b2$ represent the biases at the hidden and output layers, respectively. Figure *2.2* describes the proposed AKFNN approach, combining the AKF approach with the ANN approach.

$$w_1 = [0.43 \quad 0.19 \quad -47.28 \quad 0.36 \quad -0.43],\ w_2 = [1.70],\ b1 = [-46.62],\ b2 = [0.95]$$

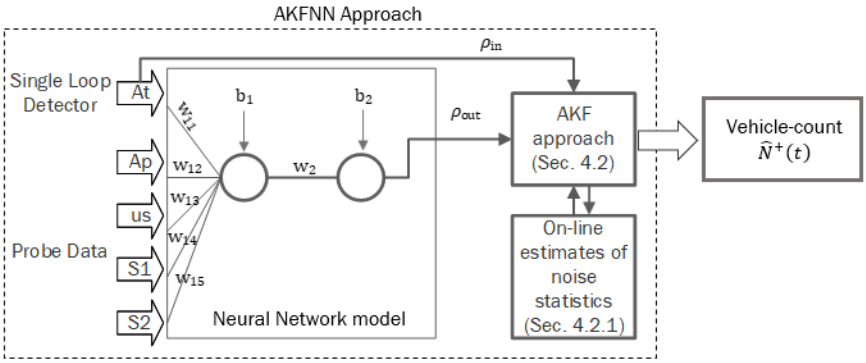

Figure 2.2 Flowchart for adaptive Kalman filter with a neural network (AKFNN) approach.

2.5. Results

This section evaluates the performance of the proposed estimation approaches. The first subsection evaluates the performance of the AKF approach and then compares the AKF with the KF (Section 2.5.1). The second subsection presents the performance of the ANN approach used for estimating the LMP of CVs at the exit of the link (ρ_{out}) (Section 2.5.2). The third subsection compares the performance of AKF with the AKFNN approach (Section 2.5.3). The fourth subsection investigates the sensitivity of the AKF estimation approach to the initial conditions (Section 2.5.4). The accuracy of the proposed approaches was evaluated based on the RMSE, as shown in Equation (41). The RMSE has been frequently used in the literature to measure the difference between the approach estimates and the actual values.

$$RMSE\ (veh)\ =\ \sqrt{\sum_{t=1}^{n}\ [\widehat{N}^{+}(t) - N(t)]^2/n} \tag{41}$$

where $\widehat{N}^{+}(t)$ represents the estimated vehicle count values, $N(t)$ represents the actual vehicle count values, and n is the total number of estimations. All simulation scenarios start with the following initial conditions: an initial vehicle count estimate of zero ($\widehat{N}^{+}(0) = 0$ veh), which is the same value as the actual vehicle count, and initial mean and the prior covariance estimates of the state system ($m(0)$ = 2 veh and $\widehat{P}^{-}(0)$= 75 veh ^{2}) if the LMP scenario is less than or equal 60%, and ($m(0)$ = 9 veh $\widehat{P}^{-}(0)$= 120 veh ^{2}) if the LMP scenario is greater than 60%. The proposed approaches were evaluated using different CV LMPs, including 10%, 20%, 30%, 40%, 50%, 60%, 70%, 80%, and 90%. For each scenario, a Monte Carlo simulation was conducted to create 300 random samples of CVs from the full data set.

2.5.1. Comparison of the KF and the AKF Approaches

This section evaluates the proposed AKF approach with real-time estimates of the error statistical parameters for the state and the measurement. This section also compares the proposed AKF with the developed KF approach in Aljamal, Abdelghaffar, and Rakha (2019b), as shown in Table 2.2. Results show that the AKF outperforms the KF approach in most scenarios except for the scenarios with high LMPs (i.e., LMP of 80% and 90%). Results demonstrate the need to provide real-time estimates for the mean and variance error values in the state and measurement when dealing with low or medium LMPs. This happened due to high error in the fixed ρ value that was used, which then produced high error in the vehicle count estimate. The AKF improved the traditional KF vehicle count estimation accuracy by up to 29%. In contrast, for high LMPs, the user may proceed with predefined statistical values for the state and measurement (mean and variance error values) due to low errors in the vehicle count estimates (low error

in the ρ value). In conclusion, a simple KF can be used with high LMPs without the need to change statistical noise parameters at every estimation step.

Table 2.2 RMSE values using KF and AKF approaches.

LMP (%)	RMSE (veh)		
	KF	AKF	Improvement (%)
10	6.0	4.3	29
20	5.6	4.0	28
30	5.0	3.8	23
40	4.6	3.6	22
50	4.1	3.6	11
60	3.6	3.2	11
70	3.0	3.0	0
80	2.3	2.6	-13
90	1.6	2.0	-25

2.5.2. Developed ANN Approach

The ANN model was employed to estimate the (ρ_{out}) value, which is used to reflect the total number of vehicle departures from the given number of CV departures. The data set was divided into 70% for training, 15% for validation, and 15% for testing. The validation data set is used to measure network generalization and to avoid any over fitting problems (Kohavi 1995). The developed ANN performance is shown in Table 2.3. The mean square error (MSE) is 0.01 and the R value is close to 1.0. The R value measures the correlation between model outputs and desired outputs. A value close to 1.0 means that the model outputs are very close to the desired outputs. Figure *2.3* shows the error histogram for the training, validation, and testing data and their deviations from the zero error bar. Most of the errors lie around the zero error bar, which means that the developed ANN model appropriately addressed the research goal (i.e., estimating ρ_{out}). Figure *2.4* presents the estimated and actual values for the ρ_{out} at different LMPs.

Table 2.3 Developed ANN model performance measures for the training, validation, and testing data set.

Data Set	Samples	MSE	*R*
Training	346,881	0.0171	0.872
Validation	74,331	0.0170	0.872
Testing	74,331	0.0173	0.871

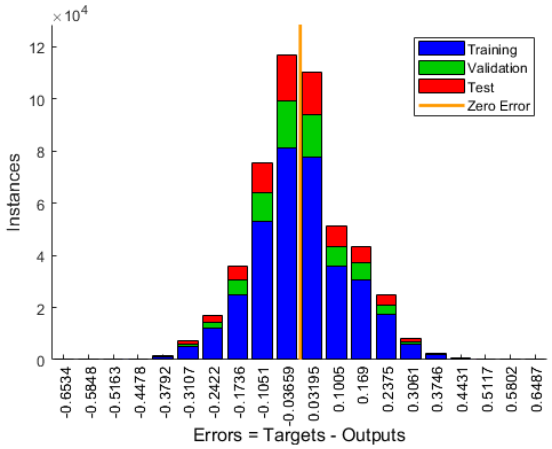

Figure 2.3 Error histogram for the training, validation, and testing data set.

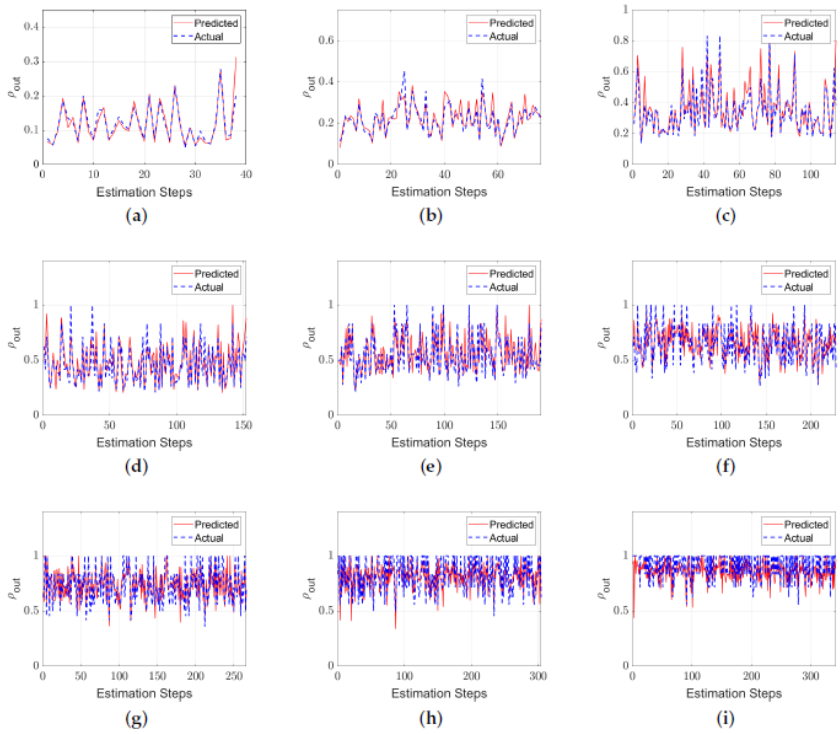

Figure 2.4 Actual and estimated values of ρ_{out} for different LMP scenarios: (a) 10%, (b) 20%, (c) 30%, (d) 40%, (e) 50%, (f) 60%, (g) 70%, (h) 80%, and (i) 90% LMP.

2.5.3. Comparison of the AKF and the AKFNN Approaches

This section demonstrates the impact of using two ρ values rather than using one predefined ρ value. The average predefined ρ value is defined as the value for the entire tested link. The average ρ value remains constant for the entire simulation for each LMP scenario. For instance, if the scenario of 10% LMP is tested, the ρ value in both the state and measurement is treated as a value of 0.1. In this chapter, we proposed the use of two ρ values; one at the entrance and one at the exit of the link to reflect the total number of arrivals and departures from the given total number of CV arrivals and departures, respectively. ρ_{in} is measured directly using the installed loop detector at the entrance of the link. The developed ANN approach

is used to estimate the ρ_{out} values. Then, the ρ_{in} and ρ_{out} values are utilized in the AKF equations. Recall that the AKF approach relies only on CV data, while the AKFNN approach uses a fusion of CV and single loop detector data.

Table *2.4* presents the RMSE values using the AKF and the AKFNN approaches. The results demonstrate the benefits of using the AKFNN approach rather than the AKF approach, where the estimation accuracy is improved by up to 26%. This finding proves what was recommended by Aljamal et al.'s previous study (Aljamal, Abdelghaffar, and Rakha 2020b) to consider two ρ values rather than one value. As a result, the proposed AKFNN approach is robust and produces reasonable errors even with low LMPs. For instance, the estimated vehicle count values are off by 3.7 veh when the LMP is equal to 10%. Figure *2.5* presents the vehicle count estimation for different LMPs using the proposed AKFNN Approach.

Table 2.4 RMSE values using the AKF and the AKFNN approaches.

LMP (%)	**RMSE (veh)**		
	AKF	AKFNN	Improvement (%)
10	4.3	3.7	13
20	4.0	3.6	11
30	3.8	3.5	9
40	3.6	3.3	8
50	3.6	2.7	26
60	3.2	2.4	25
70	3.0	2.4	20
80	2.6	2.3	12
90	2.0	1.8	10

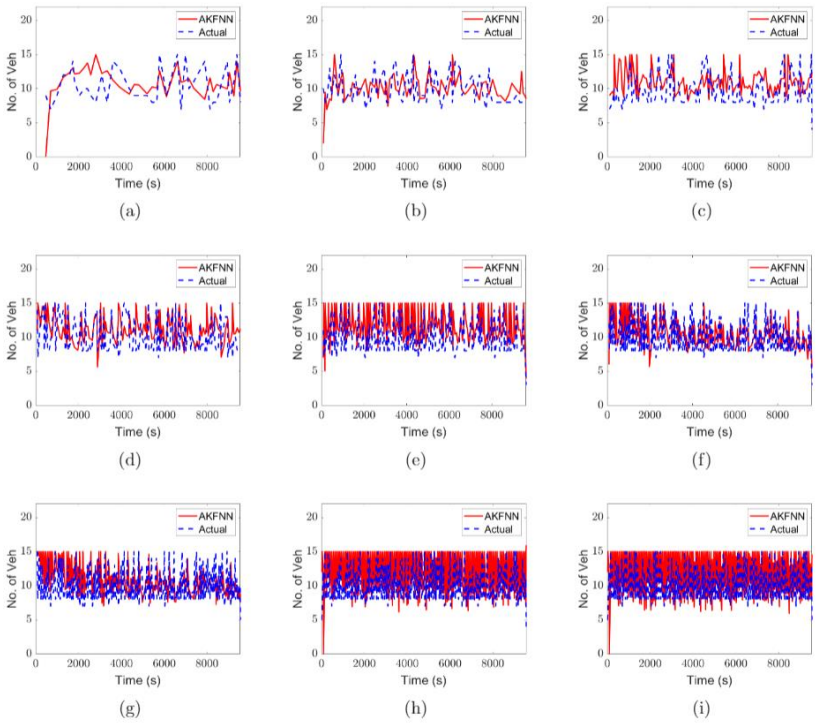

Figure 2.5 Actual and estimated vehicle counts over estimation intervals for different LMP scenarios: (a) 10%, (b) 20%, (c) 30%, (d) 40%, (e) 50%, (f) 60%, (g) 70%, (h) 80%, and (i) 90% LMP.

2.5.4. Impact of the Initial Conditions on the AKF Approach

The KF, traditional and adaptive, is sensitive to the initial condition parameters, such as the posterior state estimate ($N_i = \widehat{N}^+(0)$), the mean of state noise ($m_i = m(0)$), and the prior error covariance estimate ($P_i = \widehat{P}^-(0)$). These parameters are tuned by a trial-and-error technique to find the best initial condition values for seeking better KF estimation outcomes. However, in real applications, trial and error is not realistic and not easy to achieve. Hence, this section investigates the impact of initial conditions on the accuracy of the vehicle count estimation.

2.5.4.1. Impact of Initial Estimate of the Vehicle Count (N_i)

For the initial estimate of the vehicle count (N_i), different values were evaluated (ranging from 0 to 10 in increments of 1). In this chapter, remember that all simulation scenarios start with an initial estimate of zero ($N_i = 0$ veh), which is the same value as the actual vehicle count. Figure *2.6*a presents the RMSE values for different N_i values for the scenario of 10% LMP. As shown in the figure, the values of 8 and 10 produce the lowest RMSE. The RMSE value is equal to 4.3 veh when N_i is equal to 0. In contrast, the RMSE value is equal to 3.9 veh when N_i is equal to 8. As a result, starting the AKF approach with the best initial estimate (e.g., N_i = 8 veh) would reduce the errors and therefore improve the estimation accuracy.

2.5.4.2. Impact of Initial Mean Estimate of the State System (m_i)

Another critical initial parameter in the AKF approach is m_i. This parameter represents the mean value of the noise in the state equation. This chapter tests 16 different m_i values (i.e., $0, 1, 2, 3, 4, 5, 6, 7, 8, 9, 10$, 11, 12, 13, 14, and 15). Figure *2.6*b presents the vehicle count estimation RMSE values for different m_i values. The RMSE value is equal to 4.7 veh when the simulation starts with a 0 value of m_i. In contrast, the RMSE value is 3.9 veh when the value of m_i is equal to 11.

2.5.4.3. Impact of Initial Prior Covariance Estimate of the State System (P_i)

The last parameter tested was the initial prior estimate of error covariance P_i. The error covariance parameter describes the accuracy of the state system. For instance, if the covariance value is low, then the state outcome is accurate and close to the actual value. As stated in the literature, the initial parameters should always be tuned to achieve accurate estimation accuracy. Thirteen different P_i values were tested (i.e., $5, 10, 15, 20, 25, 50, 75, 100, 120, 150, 200$, and 250). Figure *2.6*c presents the RMSE values using different P_i values. The P_i value of 150 veh ^{2} produces the lowest RMSE values.

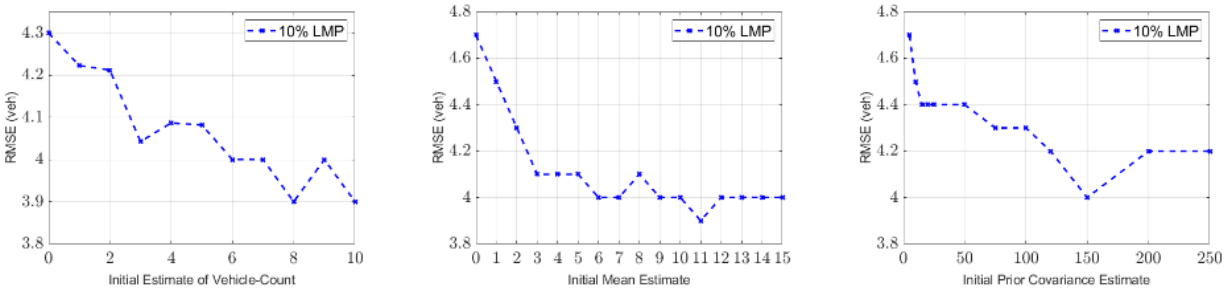

Figure 2.6 Impact of the initial conditions on the AKF approach: (a) Initial estimate values N_i, (b) Initial mean estimate values m_i, and (c) Initial covariance estimate values P_i.

The research presented in this chapter evaluates the proposed approaches as they should be in real-world applications. Therefore, the trial-and-error technique was avoided since it is not a valid solution in the field. However, it was noticed that previous research always tunes the initial parameters to determine the best initial conditions when testing their estimation approaches (Anand, Vanajakshi, and Subramanian 2011; Anand, Ramadurai, and Vanajakshi 2014; Vigos, Papageorgiou, and Wang 2008). If that is the case, let us assume that the proposed AKFNN approach always starts with the best initial value of P_i, which would produce less error. Table *2.5* presents the RMSE when considering the trial-and-error technique (Tuned AKFNN). The AKFNN and the Tuned AKFNN approaches used the same values of N_i and m_i, but they used different P_i values. N_i is assumed to be zero, while m_i has two values based on the tested scenario: a value of 2 veh when low LMP scenarios are tested (LMP $<= 60\%$), and a value of 9 veh with high LMP scenarios (LMP $> 60\%$). From the table, tuning the P_i value significantly improves the estimation accuracy for all scenarios (by up to 27%). For instance, at 10% LMP, the estimation error dropped from 3.7 to 3.3 vehicles. On the other hand, the estimated vehicle count values are off by 2.8 vehicles instead of 3.6 vehicles for the scenario of 20% LMP.

In conclusion, the AKF approach was proven to be very sensitive to the initial conditions (N_i, m_i, P_i). Hence, starting the simulation with good assumptions of the initial conditions can significantly improve the estimation accuracy, as shown in Table *2.5*. Finally, Table *2.6* presents the performance of the approaches discussed in the chapter.

Table 2.5 Impact of applying the trial-and-error technique for the initial value of covariance P_i.

LMP (%)	**RMSE (veh)**		
	AKFNN	Tuned AKFNN	Improvement (%)
10	3.7	3.3	11
20	3.6	2.8	22
30	3.5	2.7	23
40	3.3	2.4	27
50	2.7	2.1	22
60	2.4	2.1	13
70	2.4	2.1	13
80	2.3	1.8	22
90	1.8	1.5	17

Table 2.6 RMSE values for the KF, the AKF, the AKFNN, and the tuned AKFNN approaches.

LMP (%)	**RMSE (veh)**			
	KF	AKF	AKFNN	Tuned AKFNN
10	6.0	4.3	3.7	3.3
20	5.6	4.0	3.6	2.8
30	5.0	3.8	3.5	2.7
40	4.6	3.6	3.3	2.4
50	4.1	3.6	2.7	2.1
60	3.6	3.2	2.4	2.1
70	3.0	3.0	2.4	2.1
80	2.3	2.6	2.3	1.8
90	1.6	2.0	1.8	1.5

2.6. Summary and Conclusions

The chapter proposed a novel AKF approach for estimating the number of vehicles on signalized approaches using only CV data. An AKF approach was developed to provide real-time estimates of the statistical properties (mean and variance) for the state and measurement errors. The state equation is derived from the traffic flow continuity equation, while the measurement equation is constructed using the traffic hydrodynamic equation. Results show that the proposed AKF approach outperforms the traditional KF (improves the estimation accuracy by up to 29%), demonstrating the need to use real-time values of the statistical noise parameters in the KF approach.

Two estimation approaches were presented: (a) the AKF, and (b) the AKFNN. The AKF approach uses only CV data assuming a fixed LMP value that is obtained from historical data, while the AKFNN uses a fusion of CV and single loop detector data with real-time estimates of the LMP values (ρ_{in} and ρ_{out}). In this chapter, a robust ANN approach was developed to provide accurate real-time estimates of the ρ_{out} values. The selected features of the ANN approach are A_t (observed from the single loop detector), A_{CV}, u_s, S_1, and S_2 (observed from CVs).

The AKF and the ANN were combined to develop the novel AKFNN approach. Results demonstrate that the AKFNN approach significantly improves the vehicle count estimation accuracy since the ρ_{in} and ρ_{out} values are estimated better. Subsequently, the chapter compared the AKF with the AKFNN approaches, showing that the AKFNN approach outperforms the AKF, enhancing the estimation accuracy by up to 26%.

Finally, the chapter investigated the impact of the initial conditions (N_i, m_i, and P_i) on the AKF performance. Results show that the AKF approach is very sensitive to the initial conditions. For instance, starting the simulation with an N_i value of 8 instead of 0 improves the estimation accuracy by 10%. In addition, starting the simulation with an m_i value of 11 instead of 2 enhances the estimation accuracy by up to 10%. For the P_i parameter, an improvement of 7% could occur if the simulation starts with an initial value of 150 instead of 75 veh^2. The chapter also tested the accuracy of the AKFNN estimation by allowing the P_i parameter to be tuned (Tuned AKFNN approach), showing that more improvement could be achieved. Specifically, the Tuned AKFNN improves the accuracy by up to 27%. In conclusion, both approaches (AKF and AKFNN) produce high estimation accuracy when compared with the state-of-the-art KF approach.

Chapter 3. Enhancement of the Kalman Filter Approach Using a Bounded ρ in the State-Space Model

3.1. Introduction

The number of on-road vehicles has increased rapidly over the past few decades. For example, in the U.S., the number of motor vehicles registered from 1990 to 2016 increased by more than 75 million vehicles (Statista 2018), leading to serious traffic congestion in many areas. One potential approach to mitigating traffic congestion is expanding the current infrastructure by adding new lanes and roadways to accommodate growing traffic demands; however, this comes with significant associated costs. A more efficient way of solving traffic congestion is improving traffic management strategies by using advanced technologies and algorithms. Among the more recent technologies utilized for traffic management are Intelligent Transportation Systems (ITSs). ITS applications are developed to enhance transportation system efficiency, mobility, and reduce environmental impacts. In general, ITS aims at improving the infrastructure side of technology via sensors, communication, controllers, etc. Advanced Traffic Management Systems (ATMSs) constitute one ITS approach. ATMSs include advanced traffic signal control systems that optimize traffic signal timings in real-time (Rakha and Van Aerde 1995; Rakha 1995).

Traffic density is defined as the number of vehicles on a given roadway segment divided by the length of the segment (Roess, Prassas, and McShane 2011). Knowing the number of vehicles on a specific roadway segment is crucial in developing efficient adaptive traffic signal controllers; however, it is difficult to measure traffic density directly in the field. Moreover, traffic occupancy measurements from loop detectors represent a temporal estimate of the traffic stream density around the measurement location. The research described herein attempts to estimate the number of vehicles, both queued and moving, along signalized roadway links (e.g., urban roadways) using only CV data. To the authors' knowledge, this work is the first attempt to estimate vehicle counts based solely on CV data. This estimation approach will provide key input to real-time traffic signal controllers, leading to a reduction in intersection delays, vehicle emissions, and vehicle crashes.

3.2. Literature Review

Past research has used different technologies/techniques, such as loop detectors (Ghosh and Knapp 1978; Kurkjian et al. 1980; Bhouri et al. 1989; Vigos, Papageorgiou, and Wang 2008), video detection systems (Beucher, Blosseville, and Lenoir 1988), or data fusion techniques (Anand, Ramadurai, and Vanajakshi 2014; Anand, Vanajakshi, and Subramanian 2011; van Erp, Knoop, and Hoogendoorn 2017) (combining two different sources of data) to estimate the number of vehicles on signalized links. However, these techniques suffer from poor detection accuracy and have high installation costs. Emerging technologies, such as CV technology, can provide and share vehicle real-time location and speed data. These sample data can be exploited and used to estimate the traffic density without the need to install additional hardware.

Numerous studies have attempted to estimate vehicle counts. For example, Ghosh and Knoop (Ghosh and Knapp 1978) demonstrated that vehicle counts can be improved by dividing the roadway into small segments (half-mile) to produce an efficient estimation. Another study used traffic flow and occupancy data from two conventional loop detectors to estimate the number of vehicles traveling along a specific road segment using the flow continuity equation (Kurkjian et al. 1980). Vigos et al. proposed a robust algorithm that requires at least three loop detectors on a roadway segment in order to estimate the number of vehicles (Vigos, Papageorgiou, and Wang 2008); however, the cost of implementing such algorithms in the field is

high. For example, imagine that the estimation is required for a city like New York, which has almost 12,460 signalized intersections (DOT 2011). If each intersection has four approaches, it would be necessary to install 150,000 detectors in order to make a proper estimate, which is an unreasonable proposition. Bhouri et al. proposed a scalar KF in order to estimate the number of vehicles on an on-ramp section, using a recorded film to observe the density measurements (Bhouri et al. 1989), utilizing the equation of conservation of cars as a state equation. Another study measured vehicle counts by matching vehicle signatures recorded by a network of wireless magnetic sensors (Kwong et al. 2010). A video image processing algorithm of was deployed by Beucher et al., in which images were first collected from different scenes along a 150-m section, and then filters were used to detect the vehicle markers; however, this approach is difficult to utilize in the field.

Recently, data fusion has been widely used to estimate the number of vehicles along certain roadway sections, with the aim of achieving better accuracy than using only one source of data. In many of the works using data fusion, KF (Kalman 1960) was employed for estimating traffic density. One study achieved accurate estimated traffic density results using the traffic flow values measured from a video detection system and the travel time obtained from vehicle GPSs (Anand, Vanajakshi, and Subramanian 2011). The approach in this chapter is similar to that work in some aspects, but differs in two significant ways: only CV data are used and furthermore the updating time interval is considered as a variable rather than a fixed value (the updating time interval was 1 minute in (Anand, Vanajakshi, and Subramanian 2011)).

Van Erp et al. used data fusion to estimate the number of vehicles along an on-ramp segment (van Erp, Knoop, and Hoogendoorn 2017). They used traffic flow data from loop detectors and aggregated speeds from floating cars, the latter provided by Google, and set a 300-s fixed updating interval. Another study used loop detectors and CV data to estimate freeway traffic density (Qiu et al. 2010), relying on IntelliDrive technology (vehicle infrastructure integration) at a predefined updating time interval. Anand et al. used video and GPS data to estimate the number of vehicles along a roadway segment (Anand, Ramadurai, and Vanajakshi 2014). In that study, video captured the traffic flow at the segment's entrance and exit points, while GPS data provided travel time measurements.

Several researchers have used the KF technique to enhance estimates in various transportation applications, such as speed, travel time, and traffic flow. An unscented KF deployed for speed estimation using single loop detectors (Ye, Zhang, and Middleton 2006) with a nonlinear state-space equation, was able to improve the speed estimates. Another study employed a linear KF technique to estimate speed, relying on the relationship between the flow-occupancy ratio and vehicle speed (Guo, Xia, and Smith 2009), yielding acceptable speed estimates for congested traffic conditions. A cumulative travel-time responsive (CTR) real-time intersection control within a CV environment was also developed using the KF technique (Lee, Hernandez, and Stoschek 2012). In that study, the authors recommended having an LMP of at least 30% in order to realize the CTR algorithm's benefits.

In summary, the existing literature shows the benefits of using the KF technique to reduce errors and address different aspects of the traffic state estimation problem. Accordingly, the KF technique was adopted in this chapter. One commonality of the aforementioned studies is that they all estimated the number of vehicles using one source of data from fixed sensors (e.g., loop detectors) or using fused source data (e.g., video with GPS data) utilizing a predefined updating interval.

In this chapter, a scalar KF approach was applied to estimate real-time vehicle counts along signalized links using both real and simulated traffic data. This estimation technique was applied to a signalized link in downtown Blacksburg, Virginia. The proposed approach extends the state of the art in vehicle count estimates by making four major contributions:

1. This chapter defines the estimation interval as a variable rather than a fixed value. The estimation time interval is defined as the point at which exactly n CVs traversed the tested link.
2. This chapter relies only on CV data. Different CV LMPs were also tested, and recommendations for future research are presented.
3. This chapter examines the estimation accuracy when adding a single loop detector, and a sensitivity analysis is made in terms of the optimum location of the stationary sensor.
4. This chapter investigates the sensitivity of the proposed estimation model to different factors including the length of the link and the level of traffic congestion.

This chapter is organized as follows: Section 3.3 describes the estimation method and the problem formulation. Section 3.4 describes the data collected from downtown Blacksburg, Virginia. Section 3.5 shows the results of the new proposed model. Section 3.6 presents the conclusions of the chapter.

3.3. Estimation Approach

3.3.1. Define the Estimation Interval Time

Unlike other studies, this work defines the estimation time interval as a variable rather than a fixed value. This new approach enhances the estimation at low LMPs, as shown later in the Results section. For example, if the link's LMP is 10%, the number of CVs will obviously be low. If we treat the problem using a fixed estimation interval, then the probability of observing zero CVs within an interval will be high for short estimation interval durations, making the estimation inefficient and inaccurate. Accordingly, low LMPs require long intervals (e.g., 300 s) to ensure that at least one CV is on the link. In contrast, links with high LMPs can use short estimation intervals (e.g., 20 s). One of the major contributions of this chapter was to address this issue to produce an efficient and convenient way of determining the duration of the estimation period.

For this work, the updating time interval was defined as the time when an exact number of CVs traversed the link (i.e., reached the traffic signal stop bar)—reflecting a predefined sample size (n). This new approach ensures that the same number of CVs is used for each updating time interval. Thus, using this approach, the population confidence interval will be a fixed scaling of the sample confidence interval. This approach also ensures that there will be sufficient information about the CVs. Consequently, the average travel time (TT) value in Equation (54) will always be observed.

3.3.2. Formulation

This section defines the proposed formulation to estimate the total number of vehicles along a signalized link. The proposed approach utilizes the KF technique, which is comprised of two equations: (a) a state equation and (b) a measurement equation. The state equation is based on the traffic flow continuity equation as defined in Equation (42), while the measurement equation is based on the hydrodynamic relation of traffic flow given in Equation (44). The KF is a recursive estimation model that continuously repeats the state estimations and corrections. Equation (42) computes the number of vehicles by continuously adding the difference in the number of vehicles entering and exiting the section to the previously computed

cumulative number of vehicles traveling along the section. This integral results in an accumulation of error that requires fixing, and thus the need for the measurement equation.

$$N(t) = N(t - \Delta t) + \frac{\Delta t}{\rho}[q^{in}(t) - q^{out}(t)] \quad (42)$$

Here $N(t)$ is the number of vehicles traversing the link at time (t), Δt is the duration of the variable updating time interval, $N(t - \Delta t)$ is the number of vehicles traversing the link in the previous interval, q^{in} and q^{out} are the CV flows entering and exiting the link between $(t - \Delta t)$ and (t), respectively, and ρ is the LMP of CVs. The equation above produces accurate results if the scaled traffic flows (q^{in}/ρ^{in} and q^{out}/ρ^{out}) are accurate (May 1990). The total counts can be extracted from traditional loop detectors or video detection systems. We should note here that the ρ value in Equation (42) plays a major role in delivering accurate outcomes. The ρ is defined as the ratio of the number of CVs (N_{CV}) to the total number of vehicles (N_{total}), as shown in Equation (43). For instance, if ρ is 0.5, and the number of CVs is 5, then the expected total number of vehicles is 10.

$$\rho = N_{CV}/N_{total} \quad (43)$$

Equation (44) describes the hydrodynamic relationship between the macroscopic traffic stream parameters (flow, density, and space-mean speed).

$$q = ku \quad (44)$$

where q is the traffic flow (vehicles per unit time), k is the traffic stream density (vehicles per unit distance), and u is the space-mean speed (distance per unit time). The space-mean speed can be replaced using Equation (45).

$$u = D/TT \quad (45)$$

where D is the link length, and TT is the average vehicle travel time. Since CVs can share their instantaneous locations every Δt, the travel time of each CV can be computed for any road section. Thus, the CV travel time is used in the measurement equation, as shown in Equations (46), (47), and (48).

$$TT(t) = D \times \frac{k(t)}{\bar{q}(t)} \quad (46)$$

$$TT(t) = \frac{1}{\bar{q}(t)}[k(t) \times D] = \frac{1}{\bar{q}(t)}N(t) \quad (47)$$

$$TT(t) = H(t) \times N(t) \quad (48)$$

where $\bar{q}$ is the average traffic flow entering and exiting the link, and $H(t)$ is a transition vector that converts the vehicle counts to the average travel time. $H(t)$ is the inverse of the average flow (i.e., the first term of Equation (47)), as shown in Equation (49).

$$H(t) = \frac{1}{\bar{q}(t)} = \frac{2 \times \rho}{q^{in}(t) + q^{out}(t)} \quad (49)$$

The proposed estimation approach can be solved using the KF equations, as follows:

$$\hat{N}^{-}(t) = \hat{N}^{+}(t - \Delta t) + \frac{\Delta t}{\rho}[q^{in}(t) - q^{out}(t)] \quad (50)$$

$$\hat{T}T(t) = H(t) \times \hat{N}^{-}(t) \quad (51)$$

$$\hat{P}^{-}(t) = \hat{P}^{+}(t - \Delta t) \quad (52)$$

$$G(t) = \hat{P}^{-}(t)H(t)^{T}\,[H(t)\hat{P}^{-}(t)\,H(t)^{T} + R]^{-1} \quad (53)$$

$$\hat{N}^{+}(t) = \hat{N}^{-}(t) + G(t)\,[TT(t) - \hat{T}T(t)] \quad (54)$$

$$\hat{P}^{+}(t) = \hat{P}^{-}(t) \times [1 - H(t)\,G(t)] \quad (55)$$

where $\hat{N}^{-}$ is the a priori estimate of the vehicle counts calculated using the measurement prior to instant *t*, and $\hat{P}^{-}$ is the a priori estimate of the covariance error at instant t. The Kalman gain (G) is computed using Equation (53). The R variable is the covariance error of the measurements. The posterior state estimate $\hat{N}^{+}$ and the posterior error covariance estimate $\hat{P}^{+}$ are updated using Equations (54) and (55), after considering the CV travel time measurements.

It should be noted here that the ρ value in Equation (50) impacts the estimation accuracy significantly, especially for low LMPs (e.g., LMP $< 30\%$) given that it scales the estimated values. For instance, for a ρ value of 0.1, the second term of Equation (50) is scaled by a factor of 10, which results in large errors in the vehicle counts. A real illustrative example using empirical data is described in Table *3.1*. This example shows the impact of low LMPs in the state equation (i.e., ρ = 0.1). For the first estimation step, the total number of arrivals (A_T) and departures (D_T) within the polling interval are 65 and 60 as displayed in Table *3.1*, whereas the number of CV arrivals (A_{CV}) and departures (D_{CV}) for the same polling interval are 6 and 5, respectively. The first estimation starts with an erroneous initial vehicle count estimate $\hat{N}^{+}(0) = 5$ vehicles while the real number is zero as is in (Vigos, Papageorgiou, and Wang 2008). The actual total number of vehicles on the link would then be 5 vehicles $(0 + (65 - 60))$. Applying Equation (50) would produce an estimated total of 15 $(5 + (6 - 5)/0.1 = 15)$. Note that if the ρ value in Equation (50) is constrained by a lower bound, it can prevent the state equation from producing such large errors. For the same example, if the ρ lower bound in Equation (50) is set to 0.5, the total number of vehicles is estimated to be 7 $(5 + (6 - 5)/0.5)$. As can be seen from this example, the absolute error using a lower bound of 0.5 is 2 vehicles, whereas the absolute error using the estimated total counts is 10 vehicles. Consequently, it is much easier for the KF to correct a small error rather than a large error after applying the measurement equation. Figure *3.1* compares the vehicle counts using the state equation, Equation (50), with and without a lower bound on ρ, along the estimation steps for the 10% LMP scenario. It is clear that having a lower bound on ρ in the state equation improves its accuracy by reducing the distance from the actual vehicle count line (the green line in Figure *3.1*). The reason behind not allowing the market penetration to be very small is that (1) we use a single ρ value estimate to approximate the two ρ values (upstream and downstream of the link); and (2) if the ρ value is very small, the approximation error is inflated, producing a larger error in the estimated total number of vehicles. Consequently, Equation (50) can be rewritten as presented in Equation (56). The ρ factor in the state equation becomes the maximum of the historic ρ value and a lower bound (ρ_{min}), taken to be 0.5 in the analysis after examining different ρ_{min} values from 0.1 to 0.9 as presented in Table *3.2*. Note that further work is needed to develop procedures to provide more accurate estimates of the two market penetration rates; namely, the one at the entrance of the link and the one at the exit of the link.

$$\widehat{N}^{-}(t) = \widehat{N}^{+}(t - \Delta t) + \Delta t \frac{[q^{in}(t) - q^{out}(t)]}{max(\rho, \rho_{min})} \quad (56)$$

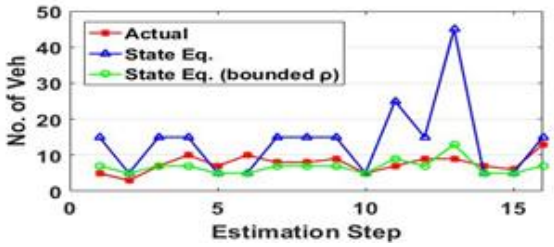

Figure 3.1 Impact of applying a lower bound in the state equation estimates.

Table 3.1 Vehicle count estimation values of using Equations (50) and (56).

Estimation Step	A_{CV}	D_{CV}	A_T	D_T	$\widehat{N}^{-}$ (Eq. 50)	$\widehat{N}^{-}$ (Eq. 56)	Actual
1	6	5	65	60	15	7	5
2	4	5	67	69	5	5	3
3	6	5	66	62	15	7	7
4	5	5	64	61	15	7	10
5	4	5	37	40	5	5	7
6	5	5	43	40	5	5	10
7	6	5	79	81	15	7	8
8	5	5	48	48	15	7	8
9	5	5	99	98	15	7	9
10	4	5	26	30	5	5	5
11	7	5	37	35	25	9	7
12	4	5	24	22	15	7	9
13	8	5	22	22	45	13	9
14	1	5	15	17	5	5	7
15	5	5	70	71	5	5	6
16	6	5	45	38	15	7	13

Table 3.2 RRMSE values using different (ρ_{min}) values in Equation (56).

LMP (%)	ρ_{min} in Equation (56)								
	0.1	0.2	0.3	0.4	0.5	0.6	0.7	0.8	0.9
10	48	45	41	40	38	38	38	37	37
20	43	43	40	39	36	35	34	33	33
30	39	39	39	38	35	33	33	32	31
40	36	36	36	36	34	30	28	27	27
50	32	32	32	32	32	29	27	26	26
60	28	28	28	28	28	28	26	24	24
70	25	25	25	25	25	25	25	22	21
80	20	20	20	20	20	20	20	20	18
90	14	14	14	14	14	14	14	14	14

3.3.3. Proposed Estimation Approaches

This section describes two estimation approaches. The first approach uses only CV data with a fixed ρ along the estimation intervals (e.g., ρ = 20%), while the second approach utilizes fused data (CV and single loop detector data), where the single loop detector provides the estimation model with actual ρ values.

3.3.3.1. First Approach: CV Data Assuming Fixed LMP (ρ)

The ρ value is an important variable in the proposed estimation approach since it scales the CV measurements to reflect the total flow. The first estimation approach uses a fixed ρ value in the estimation steps, observed from historical data. It should be noted that producing accurate estimates of the actual ρ values will produce perfect estimation outcomes as long as there are no errors in the data; the ρ values can be observed every time interval with the addition of a fixed sensor (e.g., a traditional loop detector or video detection system) to measure the total flow. The predefined ρ value in Equations (49) and (50) is computed as the arithmetic mean of all ρ observations. For instance, Figure 3.2 shows the actual ρ values versus the predefined ρ value as the red line (ρ = 20%). This figure clearly shows errors in the ρ value estimate. However, the KF reduces the errors produced from the fixed ρ assumption, as shown later in the Results section. The varying ρ values that appear in the figure are evidence that the proposed approach works well with noisy data.

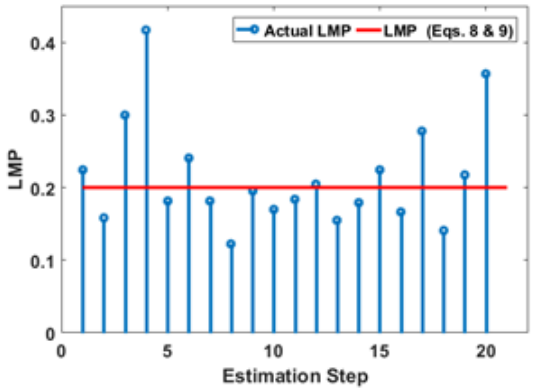

Figure 3.2 Variation in actual LMP over all the estimation intervals.

3.3.3.2. Second Approach: Fusion Data with Variable LMP (ρ)

This section employs a single loop detector in addition to CV vehicle data to estimate the LMP. The loop detector is used to observe the actual total flow and then compute the ρ values in the measurement equation for all the estimation times (t). The loop detector produces the total traffic flow, which can then be used to compute (N_{total}) in Equation (43). The new proposed estimation approach uses the same equations in the formulation section except that the measurement equation considers the actual ρ values in the H vector, as shown in Equation (57).

$$H(t) = \frac{2 \times \rho(t)}{q^{in}(t) + q^{out}(t)} \tag{57}$$

3.4. Data Collection

This chapter evaluates the proposed estimation approaches using both empirical and simulated data. This section will describe both the data and the link characteristics. The simulated data were used to provide additional data to test the KF estimator for varying conditions (e.g., traffic demand levels and link lengths).

3.4.1. Empirical Data

Figure 3.3 shows the tested link in downtown Blacksburg, Virginia. The link falls between two traffic signals. The two observer locations define the link length, as shown in Figure 3.3. The link length is approximately 74 m based on Google Maps, and the speed limit is 25 mi/h (40 km/h). The two observers

recorded the time stamp when each vehicle passed. Using the data, it was possible to conduct a Monte Carlo simulation to extract a random sample of CVs to compute (q^{in} and q^{out}) and use them in Equation (56).

The team collected actual field data for 75 minutes on March 29, 2018, between 4:00 and 5:15 p.m., observing a total of 813 vehicles. The full data served as the ground truth values, and thus our estimation approach outputs were compared to these actual values. The collected data also included the observed travel time between Observer 1 and Observer 2 (from the beginning to the end of the link). The tested link had no roadway entrances or exits between the two observers and thus the flow continuity was maintained.

Figure 3.3 Tested link in downtown Blacksburg, VA. (source: Google Maps)

3.4.2. Simulation Data

INTEGRATION (Van Aerde and Rakha 2007), a microscopic traffic simulation software, was used to validate and test the accuracy of the proposed approach. The INTEGRATION software has been extensively validated and demonstrated to replicate empirical observations. Specifically, INTEGRATION was used to create synthetic data for conditions not observed in the field to quantify the sensitivity of the proposed approach to the link length and traffic demand level. Specifically, a range of link lengths was tested (i.e., 74, 150, 200, 300, and 400 m), as shown later in the Results section. The link characteristics were calibrated to local conditions using typical values, which included a free-flow speed of 40 km/h, a speed-at-capacity of 32 km/h, a jam density of 160 veh/km/lane, and a base saturation flow rate of 1,800 veh/h/lane, which resulted in a roadway capacity of 855 veh/h given the cycle length and green times of the traffic signal. The traffic signal operated at a cycle length of 120 s and a 50:50 phase split. The amber and all-red interval was 3 s. These values were consistent with what was coded in the field.

3.5. Results and Discussion

The accuracy of the proposed KF approach was tested using real and simulated data. The evaluation of all scenarios was based on the RRMSE and the RMSE, shown in Equations (58) and (59), respectively. The two measures are frequently used in the literature to compute the difference between the approach estimates and the actual values.

$$RRMSE(\%) = 100\sqrt{S\sum_{s=1}^{S}[\hat{N}^{+}(s) - N(s)]^2 / \sum_{s=1}^{S} N(S)} \quad (58)$$

$$RMSE(veh) = \sqrt{\sum_{s=1}^{S}[\hat{N}^{+}(s) - N(s)]^2 / S} \quad (59)$$

where $N(s)$ represents the actual values, $\widehat{N}^{+}(s)$ represents the estimated vehicle count values, and S is the total number of estimations. The simulation starts with an erroneous initial estimation $\widehat{N}^{+}(0) = 5$ veh while the real number is zero as in (Vigos, Papageorgiou, and Wang 2008); the initial posterior estimate error $\hat{P}^{+}(0) = 5$, and the measurement error covariance (R) is assumed to be 5. The proposed approach was evaluated using different CV LMPs, including 10%, 20%, 30%, 40%, 50%, 60%, 70%, 80%, and 90%.

3.5.1. Empirical Data

3.5.1.1. Sample Size Impact on KF Estimator Performance

In this study, the estimation time interval was defined as the time when a prescribed number of CVs traversed the link (vehicles passed the traffic signal stop bar)—representing the desired sample size (n). This new approach ensures that the same number of CVs is used every updating estimation time interval. First, an optimal sample size (n) is needed in the estimation equations. Different sample size values were tested (i.e., 1, 2, 3, 4, 5, 6, 7, 8, 9, and 10). In the proposed approach, the sample size (n) was used to identify the estimation time step, producing a variable estimation time step. Table *3.3* presents the RRMSE values for the tested sample sizes, RRMSE values for some sample sizes are close, especially in the values between five and eight. Consequently, the sample size (n) can be different depending on the data. In this section, the optimal sample size was defined to be five; once the fifth vehicle passed the second observer, the TT variable (the arithmetic mean travel time for the five vehicles) was updated in Equation (54).

Table 3.3 RRMSE values for 10 different sample sizes for different LMPs.

Sample Size	**LMP = 10%**	**LMP = 50%**	**LMP = 80%**
1	43	34	19
2	41	32	19
3	40	33	20
4	40	33	25
5	38	32	20
6	40	32	20
7	40	32	20
8	40	33	20
9	40	37	22
10	39	38	24

3.5.1.2. Variable vs. Fixed Estimation Time Interval

Previous research always considers a constant estimation time step (e.g., 20 s). This is an appropriate approach if the entire data set is available (LMP of 100%) and/or the traffic demand is high. However, it is impossible to access the entire data set when dealing with CVs. Consequently, a variable estimation time step is used rather than a fixed one.

This section demonstrates the benefits of using variable time steps as opposed to constant values, as is done in the literature. Table 3.4 presents the RRMSE values using variable and fixed estimation time steps. The proposed variable time step method was compared to the traditional fixed interval method (i.e., 15, 20, 30, 40, 50, 60, 120, and 240 s), with the results in Table 3.4 showing that low LMPs produce infinite values from the H vector in Equation (49) in most fixed intervals. Consequently, the system produces NaN (Not a Number) values in Equation (58) due to lack of TT data.

Table 3.4 RRMSE values using variable and fixed estimation interval time periods.

Time Interval (s)	**RRMSE (%)**		
	LMP = 20%	LMP = 50%	LMP = 80%
15	NaN	NaN	NaN
20	NaN	NaN	NaN
30	NaN	NaN	91
40	NaN	NaN	96
50	NaN	NaN	43
60	NaN	57	40
120	63	49	36
240	59	60	39
Proposed Algorithm (variable time interval)	36	32	20

Table 3.5 shows the average and maximum time interval for different LMPs. The results demonstrate that low LMPs require long intervals (e.g., 300 s) to ensure that some CVs are on the approach. In contrast, links with high LMPs use short estimation intervals (e.g., 30 s). The proposed strategy ensures flexibility of the estimation intervals. Figure 3.4 shows the relationship between the sample size (n) and the average time interval for different LMPs. It should be noted here that as the sample size (n) increases, the time interval increases. This approach ensures that a sufficient number of observations are available to estimate the traffic stream density within a desired margin of error. However, a smaller sample size can be used when faster computations are needed. The user can make the trade-off between the time interval and associated error they are willing to accept. In conclusion, the proposed algorithm enhances the estimation by reducing the estimation errors and allowing the algorithm to respond more quickly for high LMPs and ensuring that sufficient observations are available to achieve the estimations for low LMPs.

Table 3.5 Estimation time interval for different LMPs.

LMP (%)	Avg Time Interval (s)	Max Time Interval (s)
10	254	450
20	131	234
30	86	177
40	66	123
50	53	111
60	43	99
70	37	101
80	33	97
90	29	78

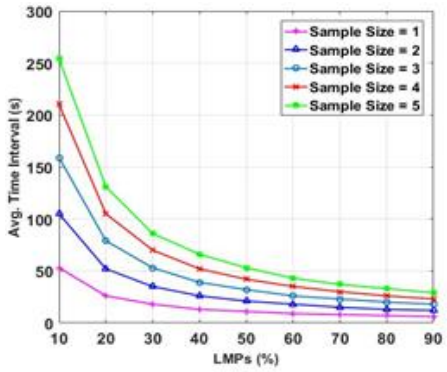

Figure 3.4 Impact of sample size on the average time interval.

3.5.1.3. 5.1. Impact of Connected Vehicle LMPs

The number of vehicles along the link was estimated considering different LMPs (i.e., 10%, 20%, 30%, 40%, 50%, 60%, 70%, 80%, and 90%). A Monte Carlo simulation was conducted to create 100 random samples from the collected data for each scenario, creating a random sample of CVs. The proposed approach used the optimal sample size obtained in the previous section ($n = 5$ veh). The more vehicle information available (i.e., the higher the LMP), the shorter the estimation interval and the more estimation steps are possible. Figure *3.5* presents the estimation along different LMPs for the empirical data. The RRMSE values produced reasonable values even with low LMPs, as shown in Table 3.6. For instance, the estimated vehicle count values are off by 2.8 vehicles when the LMP is equal to 10%. On the other hand, the estimated vehicle count values are off by 1.0 vehicles when the LMP is equal to 90%. From Table 3.6, it is clear that the error increases as the LMP decreases. It should be noted that the total field-collected data was not enough to test the KF approach accuracy at low LMPs. Thus, the model's accuracy was further tested using simulated data.

Table 3.6 RRMSE and RMSE values for nine scenarios using various LMPs for real data.

LMP (%)	RRMSE (%)	RMSE (veh)
10	38	2.8
20	36	2.6
30	35	2.5
40	34	2.4
50	32	2.3
60	28	2.0
70	25	1.8
80	20	1.4
90	14	1.0

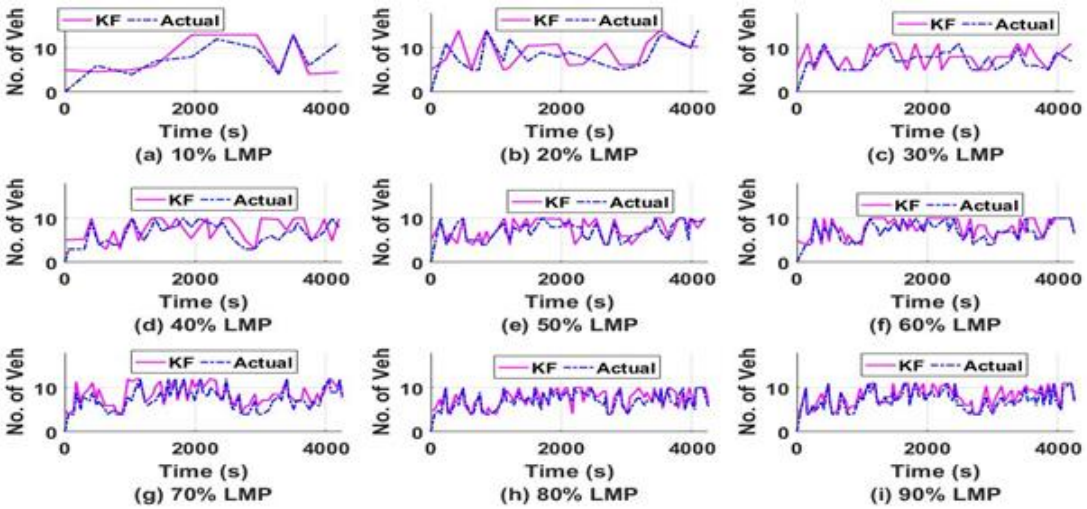

Figure 3.5 Actual and estimated vehicle counts using real data at different LMP scenarios: (a) 10%, (b) 20%, (c) 30%, (d) 40%, (e) 50%, (f) 60%, (g) 70%, (h) 80%, and (i) 90%.

3.5.1.4. Impact of Fusing Connected Vehicle and Single Loop Detector Data

This section computes the actual ρ in the measurement equation (Equation (57)) using a stationary sensor in addition to the CV data. The ρ value is defined as the ratio of the number of CVs to the total number of vehicles, as in Equation (43). Table 3.7 shows the RRMSE values using the developed two estimation approaches: (1) CV data approach assuming fixed ρ values ("CV approach"), and (2) CV and single loop detector data using variable ρ values ("fusion approach"). Different loop detector locations were tested for the fusion approach (entrance, middle, and exit) to measure the actual ρ values. Based on the RRMSE values, in some cases installing a loop detector in the middle of the tested link would slightly improve the model's accuracy at low LMPs by up to 4%; however, installing a loop detector may not be cost-effective. In conclusion, we recommend using data from existing detection sensors (e.g., loop detectors or video surveillance) if they already exist on the roads. Otherwise, we recommend using a fixed ρ value that can be estimated from historic data rather than the actual ρ.

Table 3.7 RRMSE values using one loop detector in different locations (entrance, middle, and exit).

LMP (%)	RRMSE (%)			
	CV Approach (Fixed ρ)	Fusion Approach (Variable ρ)		
		Entrance	Middle	Exit
10	38	37	34	38
20	36	35	33	36
30	35	34	32	36
40	34	34	33	34
50	32	31	31	32
60	28	28	28	28
70	25	25	24	25
80	20	19	19	20
90	14	14	12	14

3.5.2. Simulation Data

The simulation software used the same link characteristics that were observed during the data collection in downtown Blacksburg. This section first investigates the sensitivity of the vehicle count estimation approach to the link length and to the traffic demand level. Then, the simulated data were used to examine the effect of the choice of the ρ value on the estimation accuracy. First, the KF estimation approach is tested considering a constant predefined ρ in the model equations (CV approach). Second, the approach accuracy is examined using the actual ρ obtained from the installation of a single loop detector (fusion approach). In this section, the optimal sample size for simulated data was eight.

3.5.2.1. Link Length and Traffic Demand Sensitivity Analysis

First, the simulated data were used to study the sensitivity of the estimation approach to the link length. Different link lengths were investigated in addition to the original link length (i.e., 150, 200, 300, and 400 m). Table 3.8 presents the RRMSE values for different link lengths for different LMPs. The results demonstrate that the estimation accuracy increases with an increase in the link length, which is in line with Vigos et al.'s conclusion (Vigos, Papageorgiou, and Wang 2008). For the rest of this study, we used a 400-m link length to ensure that the link accommodates more vehicles.

Table 3.8 RRMSE values under different link lengths.

Link Length	LMP = 20%	LMP = 50%	LMP = 80%
74	39	37	29
150	36	30	19
200	33	26	16
300	29	22	13
400	25	21	13

Second, the impacts of traffic demand level on the estimation approach were then examined, considering both under- and over-saturated conditions. Different v/c (flow/capacity) ratios were tested (from 0.1 to 1.1 at 0.1 increments) as shown in Table 3.9. The original v/c ratio was 0.79 ($650/855 = 0.79$) based on the collected data. In general, RMSE and the RRMSE decrease with the increase of LMP for the same traffic demand level. However, the RMSE is expected to increase with increasing traffic demand levels for the same LMP, the reason being the increment in the total number of vehicles on the tested link. For instance,

at 10% LMP, for the 0.2 v/c, the RRMSE is 59% and the RMSE is 2.0, so we are off by 2.0 out of the actual 3.4 vehicles. For a 1.0 v/c ratio, the RRMSE is 24% and the RMSE is 6.5, so we are off by 6.5 vehicles out of the actual 27 vehicles. In conclusion, the RMSE value can be higher but represents better results (in our case the total number of vehicles). The results from the table demonstrate that the estimation approach works better as the level of congestion increases (e.g., v/c of 0.9, 1.0, and 1.1). The proposed approach therefore demonstrates the KF's efficiency with over-saturation scenarios (e.g., v/c = 1.1), especially for low LMPs, indicating its usefulness within a real-time traffic signal controller. Accordingly, a v/c ratio of 1.1 is used in the next section given that real-time traffic signal control is mostly needed during congested periods.

Table 3.9 RRMSE and RMSE values for different v/c ratios.

LMP (%)	**RRMSE (%), RMSE (veh)**										
	v/c=0.1	v/c=0.2	v/c=0.3	v/c=0.4	v/c=0.5	v/c=0.6	v/c=0.7	v/c=0.8	v/c=0.9	v/c=1.0	v/c=1.1
10	75, 0.8	59, 2.0	48, 2.7	43, 3.2	36, 3.4	33, 3.9	34, 4.7	29, 5.3	25, 6.3	24, 6.5	16, 5.1
20	73, 1.2	58, 1.9	45, 2.5	40, 3.1	34, 3.2	32, 3.7	29, 4.3	27, 5.0	23, 5.9	23, 6.3	14, 4.7
30	73, 1.2	55, 1.8	44, 2.4	40, 3.0	33, 3.1	29, 3.5	27, 4.0	26, 4.7	23, 5.7	22, 5.8	13, 4.4
40	73, 1.2	55, 1.8	41, 2.2	36, 2.7	30, 2.9	28, 3.3	26, 3.8	24, 4.3	21, 5.3	20, 5.4	13, 4.4
50	69, 1.2	46, 1.5	40, 2.2	33, 2.5	28, 2.7	26, 3.1	24, 3.5	22, 4.0	19, 4.8	18, 4.7	13, 4.4
60	59, 1.0	43, 1.4	35, 1.9	30, 2.3	25, 2.4	23, 2.7	20, 3.0	18, 3.4	15, 3.9	15, 4.1	12, 3.9
70	52, 0.9	42, 1.3	32, 1.8	27, 2.0	22, 2.1	20, 2.3	16, 2.4	15, 2.8	13, 3.3	13, 3.5	10, 3.4
80	48, 0.8	35, 1.2	29, 1.6	24, 1.8	19, 1.8	16, 1.9	13, 2.0	14, 2.5	11, 2.8	11, 3.0	9, 2.9
90	45, 0.8	28, 1.0	24, 1.3	22, 1.6	16, 1.5	14, 1.6	11, 1.5	11, 2.0	9, 2.2	9, 2.4	9, 2.9

In the next results sections, the simulated data were employed to examine the effect of the choice of ρ on the estimation accuracy; namely, using a constant ρ versus using the actual ρ that could be obtained if a single loop detector was installed.

3.5.2.2. Connected Vehicle Impact on KF Estimator Performance using Fixed ρ Values

The proposed KF approach was evaluated using simulation data. Again a Monte Carlo simulation was run to create 100 samples from the full data set for each scenario. In this approach, we assume the ratio between the number of CVs and the number of total vehicles is constant. The estimation equations use a predefined fixed ρ value (e.g., an average value from historical data). Table 3.10 presents the RRMSE and RMSE values using the simulation data. The RRMSE values produced reasonable values even with low LMPs, as shown in Table 3.10. For instance, the vehicle count estimates were off by 16% when the LMP equaled 10%. On the other hand, our vehicle count estimates values were off by 9% for LMPs of 90%. Furthermore, the vehicle count approach produced RMSE values of up to 5.1 vehicles. Knowing that the tested link can accommodate up to 64 vehicles based on the jam density value, these RMSE values are low. Figure *3.6* presents the estimation at different LMPs. As a result, the proposed approach addresses the research goal appropriately, producing reasonable error values. Vigos et al. considered their model robust with up to a 27.5% RRMSE using at least three loop detector measurements (Vigos, Papageorgiou, and Wang 2008). It is obvious that using the predefined ρ values results in errors. However, the KF is able to reduce these errors.

Table 3.10 RRMSE and RMSE values for various LMPs.

LMP (%)	RRMSE (%)	RMSE (veh)
10	16	5.1
20	14	4.7
30	13	4.4
40	13	4.4
50	13	4.4
60	12	3.9
70	10	3.4
80	9	2.9
90	9	2.9

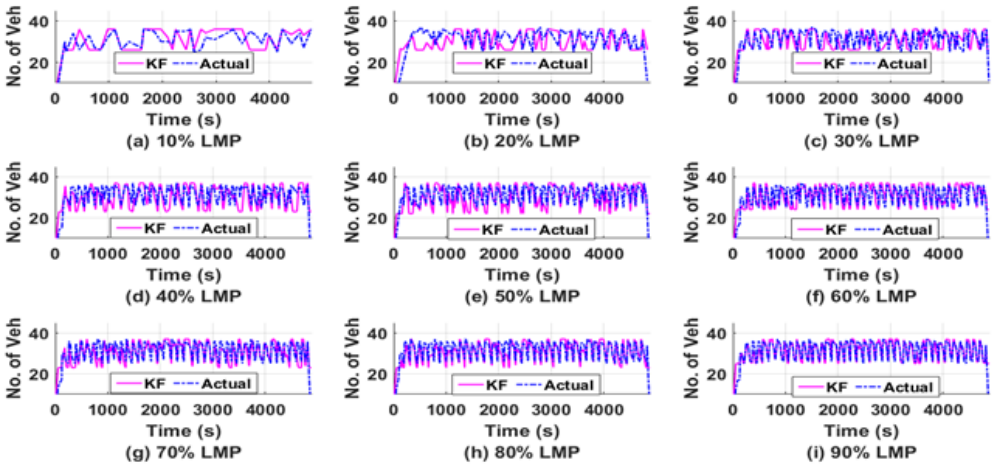

Figure 3.6 Actual and estimated vehicle counts using simulated data at different LMP scenarios: (a) 10%, (b) 20%, (c) 30%, (d) 40%, (e) 50%, (f) 60%, (g) 70%, (h) 80%, and (i) 90%.

3.5.2.3. Fusion Data Impact on KF Performance using Variable ρ Values

This section compares the two estimation approaches: The CV approach and the fusion approach. Again, different loop detector locations were tested for the fusion approach (entrance, middle, and exit) to measure the actual ρ values. The variation in the RRMSE considering a stationary sensor (e.g., loop detector) is shown in Table 3.11 for different traffic demand levels (v/c ratio of 0.2, 0.5, and 1.1). Based on the RRMSE values, in some scenarios, installing a loop detector in the middle of the tested link would slightly improve the model's accuracy by up to 8%; however, installing a loop detector may not be cost-effective. In conclusion, we recommend using a fixed ρ value that can be estimated from historic data rather than the actual ρ.

Table 3.11 RRMSE values using one loop detector in different locations (entrance, middle, and exit).

LMP (%)	V/C = 0.2				V/C = 0.5				V/C = 1.1			
	CV Approach	Fusion Approach			CV Approach	Fusion Approach			CV Approach	Fusion Approach		
		Entrance	Middle	Exit		Entrance	Middle	Exit		Entrance	Middle	Exit
10	59	55	51	53	36	35	34	37	16	15	14	15
20	58	54	51	53	34	33	33	34	14	15	15	15
30	55	53	51	53	33	32	32	33	13	14	14	14
40	55	49	50	51	30	30	30	30	13	15	15	16
50	46	47	46	48	28	27	27	28	13	14	13	14
60	43	43	43	43	25	25	25	25	12	12	12	12
70	42	39	39	40	22	21	21	22	10	10	10	11
80	35	34	34	36	19	19	20	19	9	8	8	9
90	28	27	27	28	16	16	16	16	9	9	9	9

3.6. Summary and Conclusions

This research proposed a novel approach for estimating the number of vehicles on a signalized link using CV data only. The proposed estimation approach uses a variable estimation interval that ensures a predefined number of CVs are observed in each estimation interval. The estimation equations use the linear KF technique. The state-space equation is based on the conservation equation, while the travel time measurements together with the hydrodynamic equation are used to construct the measurement equation. Two estimation approaches were presented: (a) using only the CV data to estimate the vehicle counts; this approach uses a predefined LMP value (obtained from historical data) and (b) using a single loop detector located somewhere near the middle of the section to estimate the actual LMP values. The KF estimation accuracy was evaluated using both empirical data (collected in downtown Blacksburg, Virginia) and simulated data. The work done for this chapter demonstrates the importance of having a variable estimation interval and its benefits on the estimation accuracy, especially when dealing with low LMPs. In computing the estimation interval, the algorithm first needs a certain sample size (n) to be defined. The study also investigated the sensitivity of the KF to the link length and traffic demand level, showing that the KF's relative accuracy increases as the link length increases given that the number of vehicles increases. The study also examined different demand levels (v/c ratios) in order to evaluate the KF's efficiency, with results showing that dealing with high traffic demand levels improved the estimation approach. In both estimation approaches, the results show that the estimation error increases as the LMP decreases. In some scenarios, the second approach (real-time estimated LMP) produces smaller errors since the actual LMP values can be observed. However, use of the second approach is not recommended, as it adds only slight improvements to the estimation outcomes with the additional cost associated with installing a loop detector, which may be cost prohibitive, especially in large urban areas.

Chapter 4. Development of a Particle Filter Approach

4.1. Introduction

Real-time traffic estimation has received increased attention with the introduction of advanced applications and technologies such as ITSs. Adaptive traffic signal controllers require real-time traffic state estimation to improve intersection performance, as real-time estimation plays a major role in capturing variations in traffic behavior (e.g., nonrecurrent changes). As inputs to traffic signal controllers, traffic state variables (e.g., travel time and traffic density) assist with green time allocation and help to enhance intersection performance by reducing traffic delays, vehicle emissions, and fuel consumption (Kohavi 1995). Several estimation techniques have been developed to estimate traffic state variables (Vigos, Papageorgiou, and Wang 2008; Aljamal, Abdelghaffar, and Rakha 2020b, 2019a; Mihaylova et al. 2012; Pan et al. 2013). In some previous studies, the traffic state system has been treated as a linear system (Vigos, Papageorgiou, and Wang 2008; Beucher, Blosseville, and Lenoir 1988; Aljamal, Abdelghaffar, and Rakha 2020b). Other studies have considered the system as nonlinear (Chen and Rakha 2014; Wang and Papageorgiou 2005; Mihaylova et al. 2012). For linear system models, a KF has been widely deployed to produce accurate estimates (Anand, Vanajakshi, and Subramanian 2011; Vigos, Papageorgiou, and Wang 2008; Aljamal, Abdelghaffar, and Rakha 2019a) due to its simplicity and applicability in the field. The KF assumes linear system transitions with a Gaussian distribution for the probability density function (PDF) of the system and measurement noise. For nonlinear system models, an extended KF (EKF) has been utilized in estimation (Wang and Papageorgiou 2005; Abdelghaffar, Woolsey, and Rakha 2017). The EKF also assumes that the PDF distribution is Gaussian. The EKF is derived by linearizing the system using a Taylor series expansion by calculating the Jacobian expression. However, it was found that use of the EKF approach is only valid if the system is near linearity during the updating time (Julier and Uhlmann 1997), and thus large errors may result from linearization. In addition, the task of deriving the Jacobian matrices may cause implementation difficulties (Zhai and Yeary 2004). A more robust nonlinear approach is a particle filter (PF), which has been frequently employed in the literature to handle nonlinear dynamic problems (Mihaylova et al. 2012; Wright and Horowitz 2016; Chen and Rakha 2014). The PF approach is a Monte Carlo sequential solution that deals with nonlinear system transitions without the assumption of the PDF noise distribution (Liu and Chen 1998; Ristic, Arulampalam, and Gordon 2003). In this chapter, a PF approach is developed to estimate the traffic stream density along signalized intersection approaches using only CV data. Moreover, the chapter compares the performance of the PF to the KF and adaptive KF (AKF) approaches.

Traffic density is defined as the number of vehicles per unit length on a specific roadway segment (Roess, Prassas, and McShane 2011). Estimating the traffic stream density is critical in the development of effective traffic controllers (Abdelghaffar et al. 2020). For instance in the case of freeways, identifying bottleneck locations in the early stages is critical in developing congestion mitigation strategies that include ramp metering, variable speed limits, and traffic routing. For signalized segments, the traffic density measures are crucial for either traffic signal performance (Cronje 1983; Balke, Charara, and Parker 2005; Calle-Laguna, Du, and Rakha 2019) or traffic signal optimization (Gazis and Liu 2003; Roess, Prassas, and McShane 2011). Hence, traffic density measures must be precisely estimated to represent traffic demands at each signalized intersection approach. Once accurate measurements are obtained, efficient adaptive traffic signal controllers can be developed. However, determining traffic density is not a trivial task and cannot be directly measured in the field since it is a spatial measurement. Consequently, traffic stream density is typically based on estimations. Previous research has utilized different data sources, such as

stationary sensors (e.g., loop detectors), fused data (combining two distinct data sources), and CV data to estimate traffic stream density. Traffic density estimates can be measured using video detection systems, but this is difficult due to the high cost of the infrastructure and the limited visibility of roadway segments (Vigos, Papageorgiou, and Wang 2008). Time-occupancy measurements from loop detectors are used as an alternative data source to estimate the traffic density (Cheung et al. 2005). However, time-occupancy measurements only represent the temporal density estimates around the location of the detector. A recent study introduced a relationship between time-occupancy and space-occupancy to estimate traffic density by dividing the link into small segments and installing detectors on all of the small segments (Qian, Lee, and Chung 2012), but the installation cost is high. A more common way of estimating the traffic density is the use of the traffic flow continuity equation (input-output approach), which considers two traffic counting stations, one at the entrance and the other at the end of the link (Gerlough and Huber 1976). Vigos et al. (Vigos, Papageorgiou, and Wang 2008) proposed a robust linear KF approach with at least three loop detectors to estimate the traffic density along signalized approaches. However, the implementation cost is high. Another study (Kurkjian et al. 1980) employed two conventional loop detectors to estimate the traffic density using the flow continuity equation. The two loop detectors provide the estimation model with traffic flow and occupancy data. Bhouri et al. (Bhouri et al. 1989) proposed a KF approach to estimate the traffic stream density along a freeway segment using both loop detectors and a recorded film (Bhouri et al. 1989). One commonality about the use of fixed sensors is that they are subject to detection failures and thus always produce error in their data (Lee, Hernandez, and Stoschek 2012; Mimbela and Klein 2000).

Recent research has fused different data sources to estimate the traffic stream density along certain roadway sections, increasing the accuracy of the estimate over using just one data source (Anand, Vanajakshi, and Subramanian 2011). Many works have employed the KF approach (Anand, Vanajakshi, and Subramanian 2011; Anand, Ramadurai, and Vanajakshi 2014; van Erp, Knoop, and Hoogendoorn 2017). For instance, traffic flow data at the entrance and the exit of the roadway section observed from stationary sensors together with CV data were used to estimate the traffic density (Anand, Vanajakshi, and Subramanian 2011). The CV data provided travel-time measurements to correct the prior estimate from the state equation. Another study has utilized fused loop and CV measurements to estimate the traffic density in a freeway section (Wright and Horowitz 2016). In that study, the authors derived the estimation model using the PF estimation approach, considering two sources of measurements: (1) loop detectors, and (2) fusing loop detectors and CVs. They obtained a 30% reduction in the mean absolute percentage error from the fused measurements compared to the measurements from loop detectors, demonstrating that more data sources produce more-accurate outcomes. However, the use of different data sources requires more computational cost in both time and memory as the data include both trivial (data that are not needed) and nontrivial (data that are needed) information.

Limited studies have used CV data as the only source of inputs to estimate the traffic stream density (Aljamal, Abdelghaffar, and Rakha 2020b, 2019a, 2019b). These studies developed the linear KF estimator approach. The CV data used were the number of CVs at the entry and at the exit of the tested roadway section, in addition to the travel time experienced for the CVs to traverse the tested section. Moreover, Aljamal et al. (Aljamal, Abdelghaffar, and Rakha 2020b) demonstrated that treating the estimation interval time as a variable instead of a fixed value is mandatory when dealing with only CV data, as the variable approach always ensures that sufficient information is gathered from the CVs in every estimation interval. This approach enhances the accuracy of the estimation, especially for the scenarios with a low CV LMP.

The estimation time interval for this chapter is therefore defined as the time when an exact number of CVs (i.e., 5 vehicles) reach the end of the tested link.

Several researchers have employed the PF approach to improve traffic stream estimates for different transportation applications, including traffic flow, travel time, and traffic speed. In one study, magnetic loop detectors were placed at the boundaries of the tested freeway section to estimate the traffic flow, and a PF estimation approach was developed using traffic flow and speed measurements (Mihaylova and Boel 2004). In another study, Mihaylova et al. (Mihaylova, Boel, and Hegyi 2007) developed two nonlinear approaches, an unscented KF and a PF, to produce real-time traffic flow estimates in a freeway network using data from stationary sensors. They found that the PF approach outperformed the unscented KF. Chen et al. (Chen, Rakha, and Sadek 2011) proposed a time series speed equation to estimate traffic speed. They claimed that the traffic system is nonlinear and thus presented two nonlinear approaches, a PF and an ensemble KF, using available speed measurements from loop detectors. They found that the PF approach is more accurate than the ensemble KF. Another study developed a PF estimation approach for travel-time predictions using real-time and historical data (Chen and Rakha 2014). They used the historical data to generate particles as opposed to using a state-transition model. In addition, a comparison between the PF, KF, and *k*-nearest neighbor estimators found that the PF is the most accurate approach. CV data were employed to estimate the traffic speed and flow using the PF approach (Cheng, Qiu, and Ran 2006). In that study, each link in the network was assumed to have base stations to retrieve and transfer the data. Results found that other data sources (e.g., loop detectors) should be incorporated with CV data to enhance the estimation performance. However, our recent study developed a KF approach, showing that the use of CV data alone is sufficient to obtain accurate results (Aljamal, Abdelghaffar, and Rakha 2020b).

In summary, the existing literature shows that the PF has been widely used to address nonlinear systems and has been proven to outperform other nonlinear estimation techniques; however, to our best of knowledge in the application of traffic stream density estimation, only a few studies have applied the PF approach using data from stationary sensors and fusing data from different sources. In addition, no comparison between the PF and the linear KF has been reported. Therefore, the PF was adopted in this chapter. The primary objective of this chapter is to develop a nonlinear PF estimation approach to estimate the traffic stream density based solely on CV data on signalized approaches. Subsequently, we compare the PF approach to linear estimation approaches—namely, KF and AKF—to identify the best approach for the application of the traffic density estimation, given that no comparison has been reported in the literature between these filtering techniques. Consequently, this research will recommend a specific approach to estimate the traffic stream density. The proposed three approaches are employed to estimate the vehicle counts based solely on CV data. In addition, this chapter also investigates the sensitivity of the proposed estimation approaches to several factors, such as the LMP rate of the CVs, the initial conditions, and the number of PF particles.

The chapter is organized as follows: Section 4.2 describes the problem formulation and the estimation approaches. Section 4.3 discusses the findings from applying the estimation approaches. Section 4.4 includes the conclusions of the chapter and the proposed future work.

4.2. Problem Formulation and Estimation Approaches

First, Section 4.2.1 formulates the research problem using a state-space model. Then, three different estimation approaches are described: the PF (Section 4.2.2.1), the KF (Section 4.2.2.2) and the AKF (Section 4.2.2.3).

4.2.1. State-Space Model

The state-space model is represented by a state equation and a measurement equation. The state equation describes how the system behaves and provides a priori knowledge of the estimation. The measurement equation is used to help correct and improve the prior estimation. In this chapter, the goal is to estimate the number of vehicles on signalized links using only CV data, as depicted in Figure *4.1*, where CVs are the vehicles that have the connection icon (e.g., the first vehicle on the left). The only information that is needed in practice is (1) the traffic flow of CVs observed at the tested link's entrance and exit, and (2) the travel time of each CV. V2I communication can provide this information to the traffic signal controller.

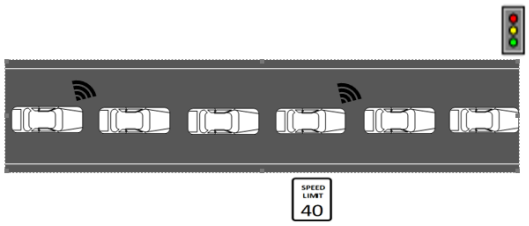

Figure 4.1 Tested link section includes CVs and non-CVs.

The model is formulated using the derived state-space equations in (Aljamal, Abdelghaffar, and Rakha 2020b). The state equation, Equation (60), is based on the continuity equation of traffic flow, whereas the measurement equation, Equation (61), is based on the traffic flow hydrodynamic relationship, based on measurements of the average travel time of the CVs. In Equation (60), the number of vehicles is computed by continuously adding the difference of the number of vehicles that enter and exit the tested section to the cumulative number of vehicles traveling along the section previously computed.

$$N(t) = N(t - \Delta t) + u(t) \tag{60}$$

$$TT(t) = H(t) \times N(t) \tag{61}$$

where $N(t)$ is the number of vehicles traversing the link at time t, $N(t - \Delta t)$ is the number of vehicles traversing the link in the preceding time interval, and $u(t)$ is the system inputs, as described in Equation (62).

$$u(t) = \frac{\Delta t\,[q^{in}(t) - q^{out}(t)]}{\max(\rho_{actual}, \rho_{min})} \tag{62}$$

where q^{in} and q^{out} represent the flow of CVs entering and exiting the link, respectively, during Δt. ρ is the CVs' LMP, defined as the ratio of CV count to total vehicle count. In the state equation, the ρ variable is set to be the maximum number of the actual ρ (ρ_{actual}) and a predefined minimum value of ρ (ρ_{min}). ρ_{actual} can be obtained from historical data. ρ_{min} is introduced to avoid producing large errors in the state equation since a single ρ value is used to approximate the two ρ values (upstream and downstream of the tested link) (Aljamal, Abdelghaffar, and Rakha 2020b). In this chapter, ρ_{min} is set to be equal to 0.5; more details about the system state representation can be found in (Aljamal, Abdelghaffar, and Rakha 2020b). It

should be noted that the ρ variable is the main noise source in the system, and thus there is an urgent need to develop the measurement equation to fix these errors. In Equation (61), TT is the average vehicle travel time, $H(t)$ is a vector that transforms the vehicle counts to travel times. $H(t)$ is derived from the hydrodynamic relationship between the macroscopic traffic parameters (flow, density, and space-mean speed), as presented in Equation (63).

$$H(t) = \frac{1}{\bar{q}(t)} = \frac{2 \times \rho_{actual}}{q^{in}(t) + q^{out}(t)} \tag{63}$$

4.2.2. Estimation Approaches

As mentioned earlier, the KF and the AKF are considered linear estimators that can efficiently handle linear state-space systems. However, in the proposed state-space equations, we suspect some nonlinearity coming from the ρ variable, which raises the question, would a nonlinear filter improve the estimation performance? For this purpose, this chapter develops a nonlinear PF approach to estimate the vehicle counts along the signalized link. This section presents the formulation of the three approaches used to estimate the vehicle counts using only CV data along signalized approaches. The three techniques are the proposed PF, the KF (Aljamal, Abdelghaffar, and Rakha 2020b), and the AKF (Aljamal, Abdelghaffar, and Rakha 2019a).

4.2.2.1. The PF Approach

The PF approach is used to solve nonlinear state-space systems with no form restrictions on the initial state and noise distributions. For instance, the PF can deal with any arbitrary PDF distribution (Liu and Chen 1998). The PF approach is used to estimate the posterior PDF of the state vehicle count variable (N) given some measurements of CV travel times (TT) by assigning k number of particles (samples). Each particle has a certain relative weight (w). When a new measurement is received, the particles' locations and weights are updated. It should be noted that the particles with low relative weight values are replaced with new particles (resampling) so that the system keeps only the important particles. The estimates are then calculated using the average value of the remaining particles. The following steps are used to implement the proposed PF approach:

1. Initialization: $t = 0$, where t is the time interval.

(a) $\widehat{N}^{+}(0)$, R, V, and l,

where $\widehat{N}^{+}(0)$ is the initial vehicle count estimate; R is the measurement's covariance error; and V is the variance of the initial vehicle count estimate, which is used to randomly generate the initial particles' locations around $\widehat{N}^{+}(0)$.

(b) Generate l particles' locations randomly, from 1 to L, from the initial prior Gaussian distribution $P(N_0)$.

$$N^{l}(0) \sim P(N_0) \tag{64}$$

2. For t = 1: T.

(a) Update the locations ($N^{l}(t)$), measurements ($TT^{l}(t)$), and weights ($w^{l}(t)$) of the particles.

$$N^{l}(t) = N^{l}(t - \Delta t) + u(t) \tag{65}$$

$$TT^{l}(t) = \ H(t) \times N^{l}(t) \tag{66}$$

$$w^{l}(t) = \frac{1}{\sqrt{2\pi R}}\ e^{-\left(TT-TT^{l}(t)\right)^{2}/2R} \tag{67}$$

where TT is the observed measurement from the CVs. The weights are then normalized using the following equation, $\widehat{w}^{l}(t) = w^{l}(t)/\sum_{l=1}^{L} w^{l}(t)$.

(b) Replace the low-weighted particles with new particles (resampling (Liu and Chen 1998)). After a few iterations in the PF process, the weight will focus on a few particles only and most particles will have insignificant weights, resulting in sample degeneracy (Li, Sattar, and Sun 2012). The resampling process is therefore used to tackle the degeneracy problem. It should be noted that the highly weighted particles are used to compute the PF posterior estimate.

(c) Compute the PF posterior estimate: The PF posterior estimate is computed as the average value of the remaining particles (particles with high weights), as shown in Equation (68).

$$\widehat{N}^{+}(t) = \frac{1}{L}\sum_{l=1}^{L} N^{l}(t) \tag{68}$$

(d) Next time step $(t + \Delta t)$: When 5 new CVs traverse the link, return to step 2a.

4.2.2.2. The KF Approach

The KF approach is a linear quadratic estimator. It has been proven to be the best for estimating linear systems with Gaussian noise (Maybeck 1990). The KF estimation approach can be solved using the following steps:

1. Initialization: $t = 0;$ where t is the time interval.

(a) $\widehat{N}^{+}(0)$, R, and $\hat{P}^{+}(0)$,

where $\hat{P}^{+}(0)$ is the initial posterior error covariance estimate for the state system.

2. For $t = 1{:}\,T$.

(a) Prior estimates:

$$\widehat{N}^{-}(t) = \widehat{N}^{+}(t - \Delta t) + u(t) \tag{69}$$

$$\hat{T}T(t) = \ H\ (t)\ \times\ \widehat{N}^{-}(t) \tag{70}$$

$$\hat{P}^{-}(t) = \ \hat{P}^{+}(t - \Delta t) \tag{71}$$

where $\widehat{N}^{-}$ is an estimate of a priori vehicle count, $\hat{T}T$ is the estimated average travel time, and $\hat{P}^{-}$ is the a priori covariance estimate for the state system.

(b) Correction: The correction uses the prior estimate and the new measurement (i.e., the CV average travel time) to compute the Kalman gain (G).

$$G(t) = \ \hat{P}^{-}(t)H(t)^{T}\ [H(t)\hat{P}^{-}(t)\ \ H(t)^{T} + R]^{-1} \tag{72}$$

(c) Posterior state estimates:

$$\widehat{N}^{+}(t) = \widehat{N}^{-}(t) + G(t)\ [TT(t) - \ \widehat{T}T\ (t)] \tag{73}$$

$$\hat{P}^{+}(t) = \hat{P}^{-}(t) \times [1 - H\ (t)\ G\ (t)] \tag{74}$$

where $\widehat{N}^{+}$ is the posterior vehicle count estimate, and $\hat{P}^{+}$ is the posterior error covariance estimate.

(d) Next time step ($t + \Delta t$): When five new CVs traverse the link, return to step 2a.

4.2.2.3. The AKF Approach

The AKF approach is presented to estimate the total number of vehicles, using real-time noise error estimates in the state and measurement systems (i.e., mean and variance values). It should be noted that the KF and the AKF approaches use the same equations, but the AKF approach dynamically estimates the noise statistical parameters every estimation step. The vehicle count estimates can be obtained using the following steps:

1. Initialization: $t = 0$; where t is the time interval.

(a) $\widehat{N}^{+}(0)$, $m(0)$, and $\hat{P}^{+}(0)$,

where $m(0)$ is the mean of the noise for the state system.

2. For t = 1: T

(a) Prior estimates:

$$\widehat{N}^{-}(t) = \widehat{N}^{+}(t - \Delta t) + u(t) + m(t - \Delta t) \tag{75}$$

$$\hat{P}^{-}(t) = \ \hat{P}^{+}(t - \Delta t) + M(t - \Delta t) \tag{76}$$

(b) Estimation of noise statistics for the measurement system:

$$\hat{T}T(t) = \ H\ (t)\ \times\ \widehat{N}^{-}(t) \tag{77}$$

$$r = \frac{1}{n}\sum_{t=1}^{n}\ [TT(t) - \hat{T}T(t)] \tag{78}$$

$$R = \frac{1}{n-1}\sum_{t=1}^{n}\ [(r(t) - r).(r(t) - r)^{T} - (\frac{n-1}{n})H(t)\hat{P}^{-}(t)H^{T}(t)] \tag{79}$$

where r and R are the mean and covariance of the measurement noise, respectively, and n is the number of state noise samples.

(c) Correction:

$$G(t) = \ \hat{P}^{-}(t)H(t)^{T}\ [H(t)\hat{P}^{-}(t)\ H(t)^{T} + R(t)]^{-1} \tag{80}$$

(d) Posterior state estimates:

$$\widehat{N}^{+}(t) = \widehat{N}^{-}(t) + G(t)\ [TT(t) - \hat{T}T(t) - r(t)] \tag{81}$$

$$\hat{P}^{+}(t) = \hat{P}^{-}(t) \times [1 - H\ (t)\ G\ (t)] \tag{82}$$

(e) Estimation of noise statistics for the state system:

$$m = \frac{1}{n}\sum_{t=1}^{n}\ [\hat{N}^{+}(t) - \hat{N}^{+}(t - \Delta t) - u(t) + m(t - \Delta t)] \tag{83}$$

$$M = \frac{1}{n-1}\sum_{t=1}^{n}\ [(m(t) - m).(m(t) - m)^{T} - (\frac{n-1}{n})\hat{P}^{+}(t - \Delta t) - \hat{P}^{+}(t)] \tag{84}$$

where m and M are the mean and covariance of the state noise, respectively.

(f) Next time step ($t + \Delta t$): When five new CVs traverse the link, return to step 2a.

4.3. Results and Discussion

This section evaluates and compares the three estimation approaches. The simulated data were generated for a signalized link under an oversaturation condition in which the traffic demand exceeds the link capacity. The free-flow speed is 40 km/h; the saturation flow rate is 1,800 veh/h/lane, resulting in a traffic capacity of 855 veh/h given the cycle length and traffic signal's green times; the speed at capacity is 32 km/h; and the jam density is 160 veh/km/lane. The traffic signal is operated at a cycle length of 120 s and a phase split of 50:50. The amber and all-red intervals are 3 s. To test the accuracy of the estimation approaches, the INTEGRATION microscopic traffic assignment and simulation software was used. The RRMSE, presented in Equation (85), was used to evaluate the proposed estimation approaches.

$$RRMSE(\%)\ =\ 100\sqrt{S\sum_{s=1}^{S}\ [\hat{N}^{+}(s) - N(s)]^{2}}/\sum_{s=1}^{S}\ N(S) \tag{85}$$

where $\hat{N}^{+}(s)$ represents the estimated count of vehicles, $N(s)$ represents the actual count of vehicles, and S is the overall number of estimations.

4.3.1. Performance of Estimation Approaches

The simulations were conducted with the same predefined initial conditions to obtain a fair comparison. The initial conditions are described in Table 4.1. It should be noted that each estimator requires specific initial variables. For instance, $\hat{N}^{+}(0)$, R, and $\hat{P}^{+}(0)$ are required for the KF approach. For all estimation approaches, the first estimate begins with an erroneous initial estimate of vehicle count ($\hat{N}^{+}(0)$ = 5 veh), whereas the actual vehicle count is zero (Vigos, Papageorgiou, and Wang 2008).

Table 4.1 Initial conditions for the KF, AKF, and PF approaches.

Initial Conditions	KF	AKF	PF
$\hat{N}^{+}(0)$ (veh)	5	5	5
R (sec ^{2})	20	–	20
V (veh ^{2})	–	–	5
L (# of part.)	–	–	200
$\hat{P}^{+}(0)$ (veh ^{2})	5	5	–
m (veh)	–	5	–

The three estimation approaches were evaluated using different CV LMPs, including 1%, 3%, 5%, 8%, 10%, 15%, 20%, 30%, 40%, 50%, 60%, 70%, 80%, and 90%. For each LMP scenario, 100 random samples from the full data set were created using a Monte Carlo simulation. Table 4.2 presents the RRMSE

values of the KF, AKF, and the PF approaches. The table indicates that estimation errors decrease with increasing LMP for all estimation approaches. The table also demonstrates that the KF outperforms the AKF and the PF approaches. For instance, for the scenario of 1% LMP, the vehicle count estimates were off by 30%, 48%, and 64% using KF, AKF and PF, respectively.

Table 4.2 RRMSE of KF, AKF, and PF approaches for different LMPs.

LMP (%)	**RRMSE (%)**		
	KF	AKF	PF
1	30	48	64
3	25	34	60
5	23	32	56
8	23	28	52
10	19	24	48
15	19	24	42
20	18	23	40
30	18	19	30
40	18	18	22
50	18	17	18
60	14	16	15
70	12	17	12
80	9	17	9
90	6	17	7

The PF approach produces high RRMSE values at low LMPs (LMP $< 40\%$), while for the high-LMP scenarios, the PF produces RRMSE values close to the values obtained from the KF. Moreover, the AKF approach produces high errors, especially at very low LMPs (LMP $< 10\%$) and high LMPs (LMP $>= 70\%$). This demonstrates that the real-time estimates of the statistical noise values obtained from the AKF are not needed for the high-LMP scenarios, and the user may proceed with predefined statistical values due to low errors in the vehicle count estimates (low error in the ρ value). It was found that the high RRMSE error values produced from the AKF and PF approaches are mainly caused from assigning an inappropriate initial vehicle count estimate, as discussed in the next section.

Figure *4.2* presents the KF, AKF, and PF estimation outcomes with regard to the actual values at different LMPs (i.e., 10% to 90% with an increase of 10% at each step). In each subfigure, three plots are generated to display the estimation approaches' outcomes with regard to the actual values; the top one displays the PF outcomes, the middle one presents the KF outcomes, and the bottom one displays the AKF outcomes. The actual curve is represented by the dotted curve. In conclusion, the KF approach is recommended, as it produces the most accurate estimates in addition to its simplicity and applicability in the field. The next section will discuss the impact of the initial conditions on the performance of the various estimation approaches.

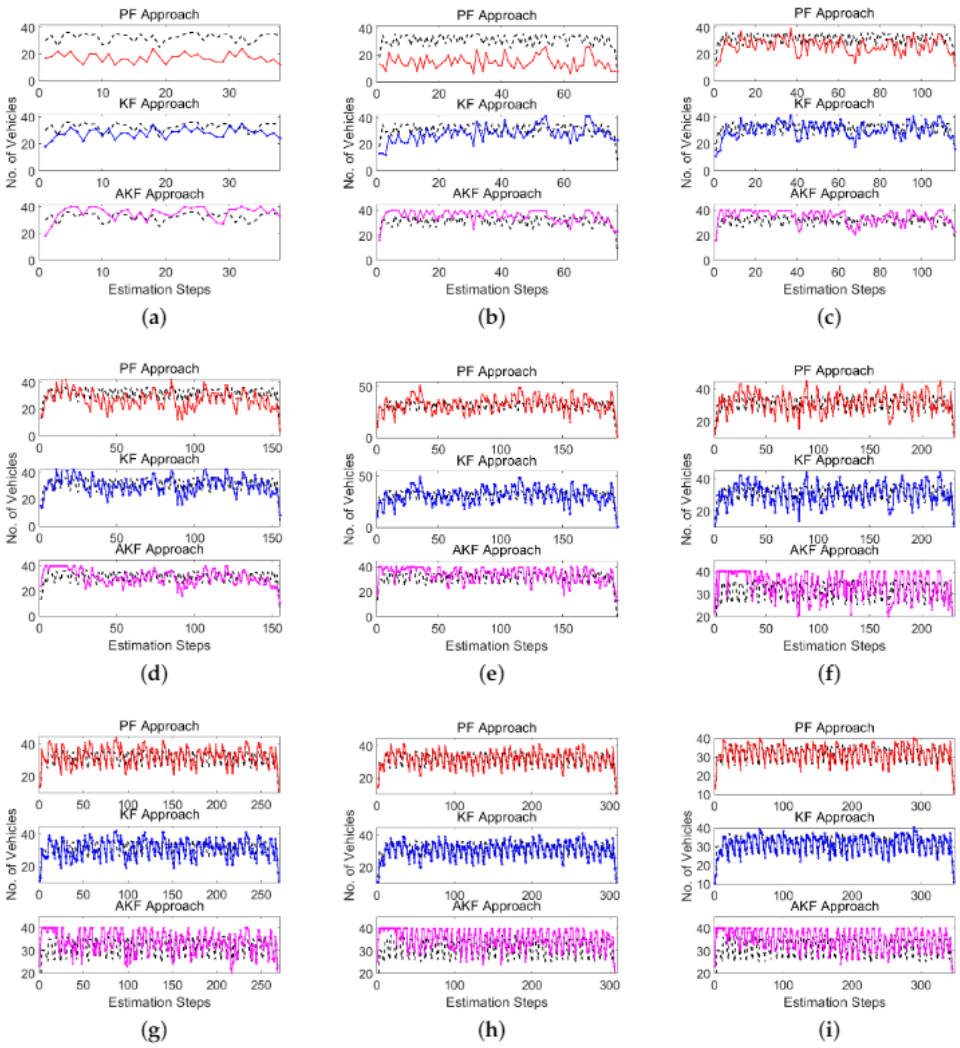

Figure 4.2 Actual and estimated vehicle counts at different LMP scenarios: (a) 10%, (b) 20%, (c) 30%, (d) 40%, (e) 50%, (f) 60%, (g) 70%, (h) 80%, and (i) 90%.

4.3.2. Impact of Initial Conditions

This section examines the effect of the choice of the initial conditions on the performance of the estimators, such as the initial vehicle count estimate $\widehat{N}^{+}(0)$ and the l number of particles in the PF approach. First, different $\widehat{N}^{+}(0)$ values were tested, from 0 to 25 at increments of 5, at different LMP scenarios, as presented in Table 4.3 and Table 4.4. Table 4.3 presents the RRMSE values when the $\widehat{N}^{+}(0)$ is set to equal 0, 5, and 10 vehicles. Table 4.4 displays the RRMSE for the $\widehat{N}^{+}(0)$ values of 15, 20, and 25 vehicles. The tables demonstrate that the RRMSE values are sensitive to the changes of the $\widehat{N}^{+}(0)$ values. The tables also show that the PF is the most sensitive estimator to $\widehat{N}^{+}(0)$ for all LMP scenarios. For instance, for the scenario of 1% LMP, the RRMSE is 81% when the simulation starts with 0 veh, while the RRMSE is 17% when $\widehat{N}^{+}(0)$ is equal to 25. Therefore, starting the simulations with an appropriate initial estimate close to the truth value significantly improves the estimation accuracy since this helps the PF to quickly converge. In addition, the AKF seems to be sensitive to the $\widehat{N}^{+}(0)$ with low LMP scenarios (LMP $<=$ 10%), while

the choice of $\widehat{N}^{+}(0)$ has a slight effect on the estimation accuracy for the scenarios with medium and high LMPs. For instance, for the scenario of 1% LMP, the RRMSE is 71% when the simulation starts with 0 veh, while the RRMSE is 21% when $\widehat{N}^{+}(0)$ is equal to 25. Lastly, the tables show that the KF is the least-sensitive estimator to the $\widehat{N}^{+}(0)$ value. Figure *4.3* summarizes the RRMSE values for nine LMP scenarios presented in Table 4.3 and Table 4.4.

Table 4.3 RRMSE values for the KF, AKF, and PF approaches using different initial vehicle count estimates (i.e., 0, 5, and 10) for different LMPs.

LMP (%)	$\widehat{N}^{+}(0) = 0$			$\widehat{N}^{+}(0) = 5$			$\widehat{N}^{+}(0) = 10$		
	KF	AKF	PF	KF	AKF	PF	KF	AKF	PF
1	34	71	81	30	48	64	27	36	51
3	28	49	78	25	34	60	23	26	47
5	26	45	73	23	32	56	23	27	44
8	24	33	69	23	28	52	23	27	41
10	19	33	62	19	24	48	20	24	37
15	21	29	55	19	24	42	20	23	37
20	20	24	47	18	23	40	19	23	35
30	19	21	34	18	19	30	19	19	27
40	18	20	24	18	18	22	19	18	19
50	19	17	18	18	17	18	17	17	22
60	14	17	14	14	16	15	15	16	19
70	12	18	12	12	17	12	12	17	17
80	9	18	9	9	17	9	9	17	15
90	6	17	6	6	17	7	7	17	14

Table 4.4 RRMSE values for the KF, AKF, and PF approaches using different initial vehicle count estimates (i.e., 15, 20, and 25) for different LMPs.

LMP (%)	$\widehat{N}^{+}(0) = 15$			$\widehat{N}^{+}(0) = 20$			$\widehat{N}^{+}(0) = 25$		
	KF	AKF	PF	KF	AKF	PF	KF	AKF	PF
1	23	32	36	20	23	24	19	21	17
3	22	26	33	20	25	24	20	24	19
5	21	25	31	20	23	26	19	24	20
8	21	27	33	22	26	26	21	26	23
10	20	24	30	20	24	27	19	26	22
15	19	23	30	19	24	26	19	23	18
20	19	23	30	19	23	30	19	23	16
30	19	19	21	19	19	21	19	19	26
40	19	18	20	19	18	20	19	18	44
50	18	17	33	18	17	47	18	17	33
60	15	16	32	15	16	32	15	16	32
70	12	17	30	12	17	30	12	17	30
80	9	17	30	9	17	30	9	17	30
90	7	17	29	7	17	44	7	17	29

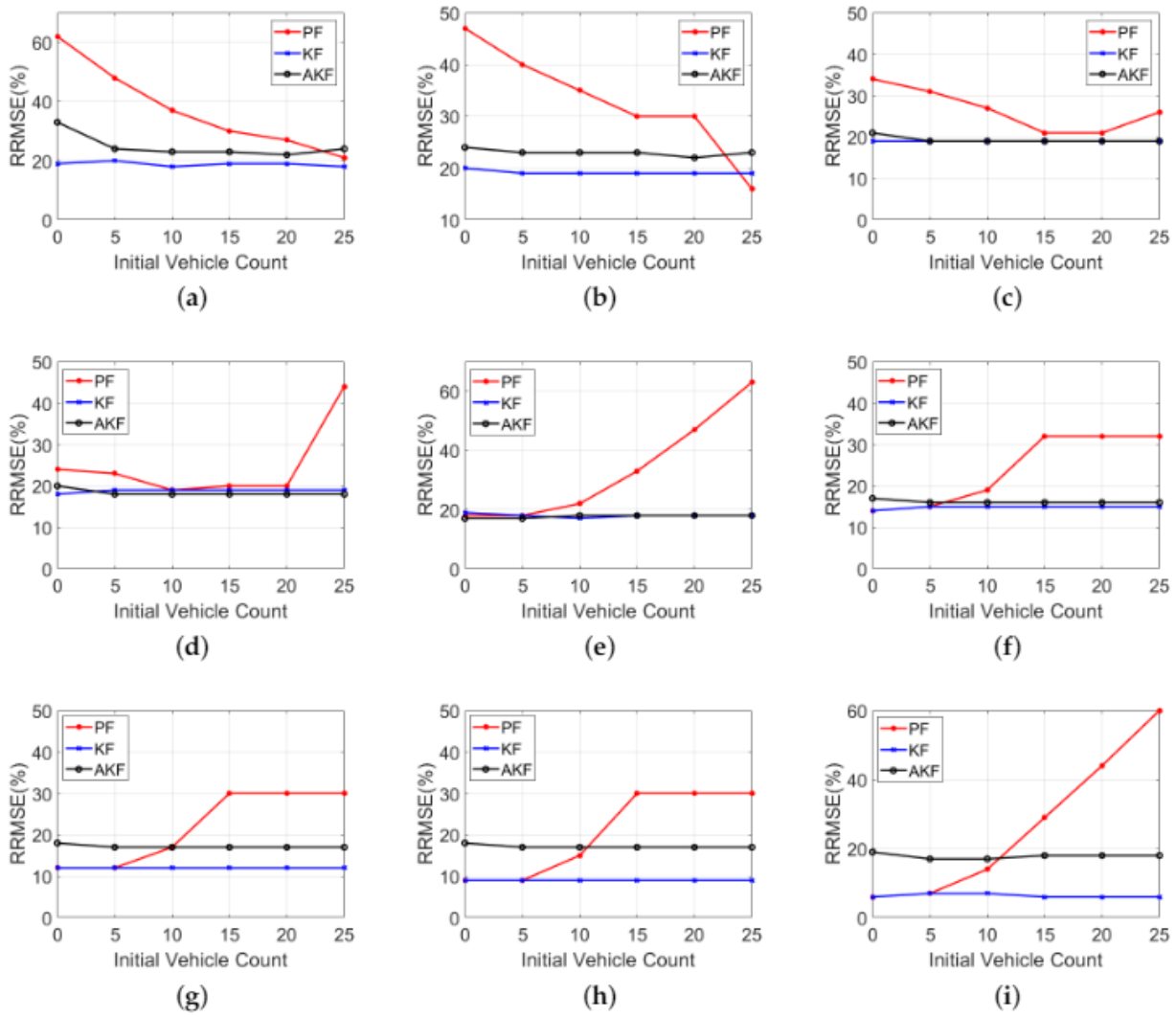

Figure 4.3 RRMSE values using various initial vehicle count estimates at different LMP scenarios: (a) 10%, (b) 20%, (c) 30%, (d) 40%, (e) 50%, (f) 60%, (g) 70%, (h) 80%, and (i) 90%.

This chapter also examined the choice of the number of particles, l, on the PF performance (i.e., $l = 10$, 100, 200, 1,000, and 2,000), as presented in Table 4.5. The findings show that the estimation accuracy increases as the number of particles increases, especially at low LMPs. However, increasing the number of particles is associated with additional computational time. The PF was implemented in MATLAB R2019a on a Dell PC with 8.0 GB RAM. The computation time ranges between 0.2 and 1.6 s, with 10 particles for various LMPs; 1.1 and 3.0 s with 100 particles; 1.3 and 6.8 s with 200 particles; 1.3 and 73 s with 1,000 particles; and 4 and 256 s with 2,000 particles. The results in Table 4.5 show that the use of 1,000 and 2,000 particles slightly reduces the RRMSE values compared to the use of 200 particles; however, this comes at a very high computational cost. Therefore, the use of 200 particles is recommended in the PF approach.

Table 4.5 RRMSE values using different number of particles in the PF for different LMPs.

LMP (%)	**RRMSE (%)**				
	l = 10	l = 100	l = 200	l = 1000	l = 2000
1	72	66	64	61	59
3	69	62	60	57	56
5	66	59	56	53	52
8	60	54	52	48	47
10	56	50	48	46	44
15	48	44	42	40	40
20	44	41	40	38	36
30	34	30	30	30	30
40	22	22	22	22	22
50	19	18	18	18	17
60	16	15	15	14	14
70	13	12	12	12	11
80	11	9	9	9	9
90	9	7	7	6	6

4.4. Summary and Conclusions

This chapter developed a nonlinear PF estimation approach to estimate the number of vehicles approaching a traffic signal based solely on CV data, with the aim of improving the estimation accuracy of linear state-of-the-art estimation approaches. This chapter introduced two linear approaches, KF and AKF, as benchmarks, to be compared with the proposed nonlinear PF approach. The results show that the KF produces the least error and accurately estimates the vehicle counts compared with the AKF and PF approaches. Consequently, to address the research problem appropriately, it is recommended to deploy the linear KF approach rather than the more complex AKF and PF approaches because of its simplicity and high-performance accuracy. In addition, the chapter investigated the sensitivity of the developed approaches to different factors, including the LMP of CVs, the initial vehicle count estimates, and the number of particles used in the PF approach. The results indicate that the estimation errors decrease as the LMP increases. Furthermore, the chapter investigated the effect of the choice of the number of particles on the performance of the PF and showed that the PF estimation accuracy increases as the number of particles increases. However, this comes at the expense of significantly longer computational times. This can significantly impact the performance of the PF, requiring longer time to converge. The results demonstrate that the KF approach is the least sensitive to the initial vehicle count estimate, while the PF approach is the most sensitive to the initial vehicle count estimate and thus is the most suitable for the proposed application.

REFERENCES

Abdelghaffar, Hossam M, Maha Elouni, Youssef Bichiou, and Hesham A Rakha. 2020. 'Development of a Connected Vehicle Dynamic Freeway Sliding Mode Variable Speed Controller', *IEEE Access*.

Abdelghaffar, Hossam M, and Hesham A Rakha. 2019. 'A novel decentralized game-theoretic adaptive traffic signal controller: large-scale testing', *Sensors*, 19: 2282.

Abdelghaffar, Hossam M, Craig A Woolsey, and Hesham A Rakha. 2017. 'Comparison of three approaches to atmospheric source localization', *Journal of Aerospace Information Systems*: 40-52.

Abdelghaffar, Hossam M, Hao Yang, and Hesham A Rakha. 2017. 'Isolated traffic signal control using nash bargaining optimization', *Global Journal of Research In Engineering*.

———. 2018. "A Novel Game Theoretic De-Centralized Traffic Signal Controller: Model Development and Testing." In.

Ajitha, T, L Vanajakshi, and SC Subramanian. 2013. 'Real-time traffic density estimation without reliable side road data', *Journal of Computing in Civil Engineering*, 29: 04014033.

Aljamal, Mohammad A, Hossam M Abdelghaffar, and Hesham A Rakha. 2019a. 'Developing a Neural–Kalman Filtering Approach for Estimating Traffic Stream Density Using Probe Vehicle Data', *Sensors*, 19: 4325.

———. 2019b. "Kalman Filter-Based Vehicle Count Estimation Approach Using Probe Data: A Multi-Lane Road Case Study." In *2019 22st International Conference on Intelligent Transportation Systems (ITSC)*. IEEE.

———. 2020a. 'Estimation of Traffic Stream Density Using Connected Vehicle Data: Linear and Nonlinear Filtering Approaches', *Sensors*, 20: 4066.

———. 2020b. 'Real-time Estimation of Vehicle Counts on Signalized Intersection Approaches Using Probe Vehicle Data', *IEEE Transactions on Intelligent Transportation Systems*.

Aljamal, Mohammad A, Hesham A Rakha, Jianhe Du, and Ihab El-Shawarby. 2018. "Comparison of Microscopic and Mesoscopic Traffic Modeling Tools for Evacuation Analysis." In *2018 21st International Conference on Intelligent Transportation Systems (ITSC)*, 2321-26. IEEE.

Anand, Asha, Gitakrishnan Ramadurai, and Lelitha Vanajakshi. 2014. 'Data fusion-based traffic density estimation and prediction', *Journal of Intelligent Transportation Systems*, 18: 367-78.

Anand, R Asha, Lelitha Vanajakshi, and Shankar C Subramanian. 2011. "Traffic density estimation under heterogeneous traffic conditions using data fusion." In *Intelligent Vehicles Symposium (IV), 2011 IEEE*, 31-36. IEEE.

Antoniou, Constantinos, and Haris N Koutsopoulos. 2006. 'Estimation of traffic dynamics models with machine-learning methods', *Transportation research record*, 1965: 103-11.

Badillo, Brian E, Hesham Rakha, Thomas W Rioux, and Marc Abrams. 2012. "Queue length estimation using conventional vehicle detector and probe vehicle data." In *2012 15th International IEEE Conference on Intelligent Transportation Systems*, 1674-81. IEEE.

Balke, Kevin N, Hassan A Charara, and Ricky Parker. 2005. "Development of a traffic signal performance measurement system (TSPMS)." In.: Texas Transportation Institute, Texas A & M University System College ….

Beucher, S, JM Blosseville, and F Lenoir. 1988. "Traffic spatial measurements using video image processing." In *Intelligent Robots and Computer Vision VI*, 648-56. International Society for Optics and Photonics.

Bhouri, Neila, Habib Haj Salem, Markos Papageorgiou, and Jean Marc Blosseville. 1989. "Estimation of traffic density on motorways." In *IFAC/IFIP/IFORS International Symposium (AIPAC'89)*, 579-83.

Calle-Laguna, Alvaro J, Jianhe Du, and Hesham A Rakha. 2019. 'Computing optimum traffic signal cycle length considering vehicle delay and fuel consumption', *Transportation Research Interdisciplinary Perspectives*, 3: 100021.

Chamberlayne, Edward, Hesham Rakha, and Douglas Bish. 2012. 'Modeling the capacity drop phenomenon at freeway bottlenecks using the INTEGRATION software', *Transportation Letters*, 4: 227-42.

Chen, Hao, and Hesham A Rakha. 2014. 'Real-time travel time prediction using particle filtering with a non-explicit state-transition model', *Transportation Research Part C: Emerging Technologies*, 43: 112-26.

Chen, Hao, Hesham A Rakha, and Shereef Sadek. 2011. "Real-time freeway traffic state prediction: A particle filter approach." In *2011 14th International IEEE Conference on Intelligent Transportation Systems (ITSC)*, 626-31. IEEE.

Cheng, Peng, Zhijun Qiu, and Bin Ran. 2006. "Particle filter based traffic state estimation using cell phone network data." In *2006 IEEE Intelligent Transportation Systems Conference*, 1047-52. IEEE.

Cheung, Sing Yiu, Sinem Coleri, Baris Dundar, Sumitra Ganesh, Chin-Woo Tan, and Pravin Varaiya. 2005. 'Traffic measurement and vehicle classification with single magnetic sensor', *Transportation Research Record*, 1917: 173-81.

Chu, Lianyu, S Oh, and Will Recker. 2005. "Adaptive Kalman filter based freeway travel time estimation." In *84th TRB Annual Meeting, Washington DC*. Citeseer.

Cronje, WB. 1983. "Analysis of existing formulas for delay, overflow, and stops." In.

Daganzo, Carlos, and CF Daganzo. 1997. *Fundamentals of transportation and traffic operations* (Pergamon Oxford).

Del Moral, Pierre. 1996. 'Non-linear filtering: interacting particle resolution', *Markov processes and related fields*, 2: 555-81.

Dion, Francois, Hesham Rakha, and Youn-Soo Kang. 2004. 'Comparison of delay estimates at under-saturated and over-saturated pre-timed signalized intersections', *Transportation Research Part B: Methodological*, 38: 99-122.

DOT, New York City. 2011. 'Traffic Signals ', Accessed 04/07. http://www.nyc.gov/html/dot/html/infrastructure/signals.shtml.

El-Tantawy, Samah, and Baher Abdulhai. 2010. "An agent-based learning towards decentralized and coordinated traffic signal control." In *13th International IEEE Conference on Intelligent Transportation Systems*, 665-70. IEEE.

Fulari, Shrikant, Lelitha Vanajakshi, and Shankar C Subramanian. 2017. 'Artificial Neural Network–Based Traffic State Estimation Using Erroneous Automated Sensor Data', *Journal of Transportation Engineering, Part A: Systems*, 143: 05017003.

Gazis, Denos, and Chiu Liu. 2003. 'Kalman filtering estimation of traffic counts for two network links in tandem', *Transportation Research Part B: Methodological*, 37: 737-45.

Gerlough, David L, and Matthew J Huber. 1976. "Traffic flow theory." In.

Ghosh, Dipankar, and CH Knapp. 1978. 'Estimation of traffic variables using a linear model of traffic flow', *Transportation Research*, 12: 395-402.

Guo, Jianhua, Jingxin Xia, and Brian L Smith. 2009. 'Kalman filter approach to speed estimation using single loop detector measurements under congested conditions', *Journal of Transportation Engineering*, 135: 927-34.

Haykin, Simon. 2007. *Neural networks: a comprehensive foundation* (Prentice-Hall, Inc.).

Jahangiri, Arash, Hesham A Rakha, and Thomas A Dingus. 2015. "Adopting machine learning methods to predict red-light running violations." In *2015 IEEE 18th International Conference on Intelligent Transportation Systems*, 650-55. IEEE.

Julier, Simon J, and Jeffrey K Uhlmann. 1997. "New extension of the Kalman filter to nonlinear systems." In *Signal processing, sensor fusion, and target recognition VI*, 182-93. International Society for Optics and Photonics.

Kalman, Rudolph Emil. 1960. 'A new approach to linear filtering and prediction problems', *Journal of basic Engineering*, 82: 35-45.

Khan, Sakib Mahmud, Kakan C Dey, and Mashrur Chowdhury. 2017. 'Real-time traffic state estimation with connected vehicles', *IEEE Transactions on Intelligent Transportation Systems*, 18: 1687-99.

Kohavi, Ron. 1995. "A study of cross-validation and bootstrap for accuracy estimation and model selection." In *Ijcai*, 1137-45. Montreal, Canada.

Kurkjian, Andrew, Stanley B Gershwin, Paul K Houpt, Alan S Willsky, EY Chow, and CS Greene. 1980. 'Estimation of roadway traffic density on freeways using presence detector data', *Transportation Science*, 14: 232-61.

Kwong, Karric, Robert Kavaler, Ram Rajagopal, and Pravin Varaiya. 2010. 'Real-time measurement of link vehicle count and travel time in a road network', *IEEE Transactions on Intelligent Transportation Systems*, 11: 814-25.

Lee, Jonathan, Marcial Hernandez, and Arne Stoschek. 2012. "Camera system for a vehicle and method for controlling a camera system." In.: Google Patents.

Lee, Joyoung, Byungkyu Park, and Ilsoo Yun. 2013. 'Cumulative travel-time responsive real-time intersection control algorithm in the connected vehicle environment', *Journal of Transportation Engineering*, 139: 1020-29.

Li, Tiancheng, Tariq Pervez Sattar, and Shudong Sun. 2012. 'Deterministic resampling: unbiased sampling to avoid sample impoverishment in particle filters', *Signal Processing*, 92: 1637-45.

Liu, Jun S, and Rong Chen. 1998. 'Sequential Monte Carlo methods for dynamic systems', *Journal of the American statistical association*, 93: 1032-44.

May, Adolf D. 1990. 'Tra c Flow Fundamentals', *University of California, Berkeley, Prentice-Hall, Inc., New Jersey*.

Maybeck, Peter S. 1990. 'The Kalman filter: An introduction to concepts.' in, *Autonomous robot vehicles* (Springer).

Mihaylova, Lyudmila, and René Boel. 2004. "A particle filter for freeway traffic estimation." In *2004 43rd IEEE Conference on Decision and Control (CDC)(IEEE Cat. No. 04CH37601)*, 2106-11. IEEE.

Mihaylova, Lyudmila, René Boel, and Andreas Hegyi. 2007. 'Freeway traffic estimation within particle filtering framework', *Automatica*, 43: 290-300.

Mihaylova, Lyudmila, Andreas Hegyi, Amadou Gning, and René K Boel. 2012. 'Parallelized particle and Gaussian sum particle filters for large-scale freeway traffic systems', *IEEE Transactions on Intelligent Transportation Systems*, 13: 36-48.

Mimbela, Luz Elena Y, and Lawrence A Klein. 2000. 'Summary of vehicle detection and surveillance technologies used in intelligent transportation systems'.

Myers, Kenneth, and BD Tapley. 1976. 'Adaptive sequential estimation with unknown noise statistics', *IEEE Transactions on Automatic Control*, 21: 520-23.

Pan, TL, Agachai Sumalee, Ren-Xin Zhong, and Nakorn Indra-Payoong. 2013. 'Short-term traffic state prediction based on temporal–spatial correlation', *IEEE Transactions on Intelligent Transportation Systems*, 14: 1242-54.

Press, S James, and Kazuo Shigemasu. 1989. 'Bayesian inference in factor analysis.' in, *Contributions to probability and statistics* (Springer).

Qian, Gongbin, Jinwoo Lee, and Edward Chung. 2012. 'Algorithm for queue estimation with loop detector of time occupancy in off-ramps on signalized motorways', *Transportation Research Record*, 2278: 50-56.

Qiu, Tony, Xiao-Yun Lu, Andy Chow, and Steven Shladover. 2010. 'Estimation of freeway traffic density with loop detector and probe vehicle data', *Transportation Research Record: Journal of the Transportation Research Board*: 21-29.

Rakha, H, P Pasumarthy, and S Adjerid. 2004. 'The INTEGRATION framework for modeling longitudinal vehicle motion', *TRANSTEC: Athens, Greece*.

Rakha, H, and M Van Aerde. 1995. 'REALTRAN: an off-line emulator for estimating the effects of SCOOT', *Transportation research record*: 124-28.

Rakha, Hesham Ahmed. 1995. 'A simulation approach for modeling real-time traffic signal controls'.

Rakha, Hesham, Youn-Soo Kang, and François Dion. 2001. 'Estimating vehicle stops at undersaturated and oversaturated fixed-time signalized intersections', *Transportation Research Record*, 1776: 128-37.

Ristic, Branko, Sanjeev Arulampalam, and Neil Gordon. 2003. *Beyond the Kalman filter: Particle filters for tracking applications* (Artech house).

Roess, Roger P, Elena S Prassas, and William R McShane. 2011. *Traffic engineering* (Pearson Education, Inc.: Hoboken, NJ, USA).

Roweis, Sam. 1996. 'Levenberg-marquardt optimization', *Notes, University Of Toronto*.

Sekuła, Przemysław, Nikola Marković, Zachary Vander Laan, and Kaveh Farokhi Sadabadi. 2018. 'Estimating historical hourly traffic volumes via machine learning and vehicle probe data: A Maryland case study', *Transportation Research Part C: Emerging Technologies*, 97: 147-58.

Shahrbabaki, Majid Rostami, Ali Akbar Safavi, Markos Papageorgiou, and Ioannis Papamichail. 2018. 'A data fusion approach for real-time traffic state estimation in urban signalized links', *Transportation research part C: emerging technologies*, 92: 525-48.

Statista. 2018. 'Number of motor vehicles registered in the United States from 1990 to 2016 (in 1,000's)', Accessed 05/07. https://www.statista.com/statistics/183505/number-of-vehicles-in-the-united-states-since-1990/.

Teply, Stan. 1985. *Highlights of the Canadian capacity guide for signalized intersections* (TRB).

Van Aerde, M, and H Rakha. 2007. 'INTEGRATION© Release 2.30 for Windows: User's Guide–Volume II: Advanced Model Features', *M. Van Aerde & Assoc., Ltd., Blacksburg2007*.

van Erp, Paul BC, Victor L Knoop, and Serge Hoogendoorn. 2017. "Estimating the Vehicle Accumulation: Data Fusion of Loop-Detector Flow and Floating Car Speed Data." In *TRB*. Washington, D.C., US.

Vigos, Georgios, Markos Papageorgiou, and Yibing Wang. 2008. 'Real-time estimation of vehicle-count within signalized links', *Transportation Research Part C: Emerging Technologies*, 16: 18-35.

Wang, Yibing, and Markos Papageorgiou. 2005. 'Real-time freeway traffic state estimation based on extended Kalman filter: a general approach', *Transportation Research Part B: Methodological*, 39: 141-67.

Wassantachat, Thanes, Zhidong Li, Jing Chen, Yang Wang, and Evan Tan. 2009. "Traffic density estimation with on-line SVM classifier." In *2009 Sixth IEEE International Conference on Advanced Video and Signal Based Surveillance*, 13-18. IEEE.

Wright, Matthew, and Roberto Horowitz. 2016. 'Fusing loop and GPS probe measurements to estimate freeway density', *IEEE Transactions on Intelligent Transportation Systems*, 17: 3577-90.

Ye, Zhirui, Yunlong Zhang, and Dan Middleton. 2006. 'Unscented Kalman filter method for speed estimation using single loop detector data', *Transportation Research Record: Journal of the Transportation Research Board*: 117-25.

Zhai, Y, and M Yeary. 2004. "Implementing particle filters with Metropolis-Hastings algorithms." In *Region 5 Conference: Annual Technical and Leadership Workshop, 2004*, 149-52. IEEE.

Zmud, Johanna, Ginger Goodin, Maarit Moran, Nidhi Kalra, and Eric Thorn. 2017. 'Advancing Automated and Connected Vehicles'.